2009

Islanded operation of a distribution feeder with distributed generation

Chandu Venu
University of Nevada Las Vegas

ISLANDED OPERATION OF A DISTRIBUTION FEEDER WITH DISTRIBUTED GENERATION

by

Chandu Venu

Bachelor of Technology in Electronics and Communication Engineering
Jawaharlal Nehru Technological University, India
May 2007

A thesis submitted in partial fulfillment
of the requirements for the

Master of Science Degree in Electrical Engineering
Department of Electrical and Computer Engineering
Howard R. Hughes College of Engineering

Graduate College
University of Nevada, Las Vegas
Decemeber 2009

UNLV
UNIVERSITY OF NEVADA LAS VEGAS

THE GRADUATE COLLEGE

We recommend that the thesis prepared under our supervision by

Chandu Venu

entitled

Islanded Operation of a Distribution Feeder with Distributed Generation

be accepted in partial fulfillment of the requirements for the degree of

Master of Science
Electrical Engineering

Yahia Baghzouz, Committee Chair

Paolo Ginobbi, Committee Member

Yingtao Jiang, Committee Member

Laxmi P. Gewali, Graduate Faculty Representative

Ronald Smith, Ph. D., Vice President for Research and Graduate Studies
and Dean of the Graduate College

December 2009

ABSTRACT

Islanded Operation of a Distribution Feeder with Distributed Generation

by

Chandu Venu

Dr. Yahia Baghzouz, Examination Committee Chair
Professor, Electrical and Computer Engineering,
University of Nevada, Las Vegas

A distribution system that is equipped with distributed generators, such as roof-mounted photovoltaic systems, can operate as a microgrid (i.e., separated from the grid) under some specific conditions. A key feature of a microgrid is its ability to separate and isolate itself from the utility seamlessly with little or no disruption to the loads within the microgrid. Then, when the utility grid returns to normal, the microgrid automatically resynchronizes and reconnects itself to the grid, in an equally seamless manner. This thesis addresses the conditions necessary for proper microgrid operation: these include local generation-load mismatch, local energy storage, load switching, and voltage and frequency control. Computer simulations using Matlab/Simulink will be conducted under various scenarios to validate such necessary conditions.

ACKNOWLEDGMENTS

I am extremely happy to take this opportunity to acknowledge my debts and gratitude to those who were associated with the preparation of this thesis. Words fail to express my profound regards from the inmost recess of my heart to my advisor Dr. Yahia Baghzouz for the invaluable help, constant guidance and wide counseling extended to me right from the selection of the research topic to the successful completion of this thesis. Academic assistance apart, I would like to thank him sincerely for his infinite patience which was one of the driving forces for me to successfully complete this thesis.

I am extending my sincere thanks to Dr. Yingtao Jiang , Dr. Paolo Ginobbi, Dr. Laxmi Gewali for their direct and indirect contribution throughout this investigation. I owe deepest gratitude to my friend Reshma Koganti without whom, this thesis would not have been possible. I would like to give special thanks to my parents and brother for their continuing love and affection throughout my life and career. Finally, I am indebted to my colleagues, Rakesh Choudary Malepati, Rohit Reddy Saddi, Anup Kumar Miryala and Aditya Chainulu karamcheti, Varun Reddy Seva for their help, support, interest and allowing me to concentrate major part of my time on thesis.

LIST OF FIGURES

TABLE OF CONTENTS

CHAPTER 1

INTRODUCTION

1.1. Introduction

Recent developments in the electric utility industry are encouraging the entry of power generation and energy storage at the distribution level [1]-[6]. Together, they are identified as distributed generation units. Several new technologies are being developed and marketed for distributed generation, with capacity ranges from a few kW to 10 MW [3]. The distributed generation includes photovoltaic systems, wind energy systems, diesel engines, micro turbines, fuel cells and gas turbines and battery storage systems.

The major interest in distributed generation systems is mainly concentrated on onsite generations [7]. The main reason contributing to this is the fact that huge power plants cannot be established in many areas due to economic factors, environmental regulations etc. Moreover with technological advancements in power electronics, energy storage devices at distribution level have created a further incentive to utilize the distributed generation systems [7]-[9]. The various distributed generation systems mentioned above can be applied for systems such as standalone, standby, grid interconnected, cogeneration and peak shavings etc. These systems provide an environmental friendly way of power generation with increased reliability, high power quality, uninterruptible power generation, cost savings and expandability.

Enabling the penetration of distributed generators into an electrical power grid is a smart option for power utility companies and customers. This is due to the fact that distributed generation systems help in improving the power quality, power supply flexibility, increasing system stability, optimizing the distribution system and reducing

the costs. A grid consisting of power utility, distributed generation systems and load can be called a microgrid or smart grid. An individual microgrid will be able to sustain on its own and possess the ability to bear the local load inspite of power outage from the utility grid.

1.1.1. Microgrids

The Microgrid [MG] concept assumes a cluster of loads and distributed generators that operate as a single controllable system that provides power to its local area [10]-[14]. This concept provides a new paradigm for defining the operation of distributed generation.

A Microgrid consists of a group of radial feeders, which could be part of a distribution system. There is a single point of connection to the utility called point of common coupling [PCC]. The feeders also have the distributed generators consisting of a photovoltaic [PV] or wind turbine [WT] or a fuel cell [FC] or diesel generator [DG] or/and battery storage [14], [15]. The static switch [SD] is used to island feeders from the utility when an outage occurs. To serve the load demand, electrical power can be produced either directly by any of the above mentioned distributed generation systems. The use of distribution systems with other fuel types can be modeled by changing the system parameters to reflect the change in the fuel consumption characteristics [e.g. fuel heating values, and efficiency of the engines].

1.1.2. Islanding

In a distribution system, when a Utility grid is disconnected for any reason, the distributed generation still supplies the required power to any section of local loads. phenomenon is called “Islanding Phenomena”. When an islanding occurs, the voltages

and frequencies in the islanded area cannot be controlled by the grid system [11][12][14]. This may lead to damage of electrical equipments and pose a danger to the working personnel. To avoid the occurrence of islanding phenomena, many control schemes have been proposed and devised to sense the islanding. Research and studies have shown that if inverters from multiple manufacturers were to be installed causes a decrease in detecting the islanding phenomena [12]. A basic distribution system consists of a Distributed Generators such as Photo voltaic panels, Wind turbines and/or other forms of renewable energy. As these renewable sources produce a Direct current, a DC-AC inverter is needed to convert the Direct current to an Alternating current with the right frequency and harmonics in relative to the AC coming out of the utility grid [10]. A battery storage system [BSS] can be inculcated into the system to store the excess energy, if produced.

Islanding once again can be classified into two types namely:

(i) Unintentional Islanding

(ii) Intentional Islanding

(i) Unintentional islanding: As the name suggests is an undesirable islanding caused in a power grid. It occurs when a part of the distribution system becomes electrically isolated from the whole power grid and is still being energized by the distributed generators. The reason for such occurrence of islanding is due to several reasons such as inverter misinterpreting the voltage and frequency harmonics of utility grid, ground fault on the feeder from grid etc. During a steady state, the real and reactive power produced by the distributed generators and the utility grid should match with the consumption.

Any mismatch in real power gives rise to frequency deviation [24]. A part of the grid with balanced load and generation may become islanded when there is a sudden opening of switch or a circuit breaker. Also when such islanding takes place, the working personnel are not aware of the power present in the microgrid and therefore may have a danger of being electrocuted. Also the distributed generators in the islanded microgrid can be damaged if the island is reconnected to the utility grid as the distributed systems usually tend to operate at a different frequency in the islanded mode and could be out of synchronism with the utility grid. This may also give rise to high starter currents which in turn may once again result in tripping of the utility system.

(ii) Intentional Islanding: Intentional islanding can be explained as a purposeful islanding of a microgrid from the remaining power grid system. When there is a power outage, many distributed generators may go out of synchronous with one another and therefore it is required to have specific islands at points where there is a slight mismatch between load and generation. Circuit breaking operations are executed to develop islanded systems.

The inverter developed in this thesis is a grid tie inverter. It is used in distributed generation systems to convert the direct current [DC] from the distributed generators into an alternating current [AC] and supply it to the load and utility grid. From a business point of view, the residences and buildings that own a grid tied electrical system are allowed to sell the energy developed by their system to the utility grid.

Under normal conditions, the grid tie inverters shut off if they detect the absence of utility grid. But, if the load which is connected to the grid starts resonating to the

frequency of utility grid, the inverter will fail to detect the absence and causes islanding [18]-[23]. Therefore the inverter should be designed for a grid tie operation which has an anti islanding protection embedded in it. Anti islanding protection usually fires minute pulses which are out of phase with the utility grid cancelling any undesired resonances.

Inverter sees to that the active power [P] and reactive power [Q] supplied by the distributed generators are equal to the active power and reactive power demanded by the loaded under both normal mode and islanded mode. Under a normal mode, when the load is connected to the utility grid and distribution system, the inverter provides a part power demanded by the load [19]. When a grid is islanded, the inverter must have the ability to increase the power supply from the distribution system in negligible amount of time to sustain the sudden increase in the load demand.

Care should be taken such that, when the utility grid breaks off from the load, the power from the distributed generation should be supplied to the load without any major hindrances to the voltage and frequency parameters of the grid system. And, when the utility grid is connected to the load, the distribution system should allow the load to re-connect itself to the grid in an equally error-free manner. This grid connected distributed systems is simulated using Matlab/Simulink blocks [13].

To simply the entire system a DC voltage source acts as a photo-voltaic panel, while the DC-DC boost is used to maintain the Maximum power point tracking. The DC-AC inverter is modeled using a universal bridge consisting of IGBTs. A pulse width generator with an external source of sinusoidal wave input is used to provide the firing pulses to switch the alternating gates of the universal bridge [19]-[21]. The resultant PWM wave from the inverter in converted to a sinusoidal wave using a LC filter. Care is

taken that, the frequency of this resultant sine wave is in order with the sinusoidal wave from the utility grid. The load utilized here is a resistive and inductive load, RL, in parallel to the distributed generation system and utility grid [18]. A programmable switch is used to island the load system from the utility grid.

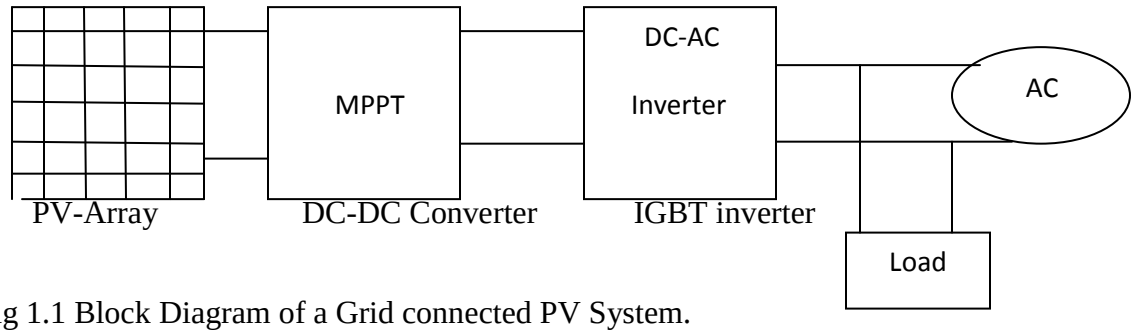

Fig 1.1 Block Diagram of a Grid connected PV System.

1.1.3. Reasons for Microgrids

The conventional arrangement of a modern large power system offers a number of advantages. Large generating units can be made efficient and operated with only a relatively small number of personnel [7]-[9]. The interconnected high voltage transmission network allows the generator reserve requirement to be minimized, the most efficient generating plant to be dispatched at any time, and bulk power to be transported large distances with limited electrical losses. The distribution network can be designed for unidirectional flow of power and sized to accommodate customer loads only. However, over the last few years a number of influences have combined to lead to the increased interest in Microgrid schemes [10]. These can be listed as reduction in gaseous emissions (mainly CO_2), energy efficiency or rational use of energy, deregulation or

competition policy, diversification of energy sources, national and global power requirements.

The other reasons with additional emphasis on commercial considerations are availability of modular generating plants, ease of finding sites for smaller generators, Short construction times and lower capital costs of smaller plants, generating may be sited closer to load, which may reduce transmission costs.

1.2. Stimulus for Microgrids

Currently a lot of research is being undertaken into Microgrids. Although components of the Microgrids are fairly well understood, the system as a whole is not. When several sources are connected to form a Microgrid, the system behavior is unpredictable. This being the case, modeling the system and simulating it, in order to develop an appropriate management system, are the heart of micro-grid research. Nowadays, several research groups around the world are investigating the feasibility and benefits that the Microgrids may provide. Some problems are encountered including dealing with the unbalanced loads and harmonics associated with the system. Modeling is an important component for power system energy management system. A precise model helps the electric utility to make unit commitment decisions and to reduce operating costs and emission level properly. Besides playing a key role in meeting the load demand, it is also essential to maintain the reliability of the Microgrid. This thesis focuses on the modeling of Microgrids, and conditions required for a microgrid to dynamically synchronize itself with the Utility grid and load and resynchronize when the Islanding phenomena occurs.

1.3. Management of Microgrid

Significant research is currently carried out regarding the operation and control of Microgrids. The emphasis lies on the following parameters:

1) Optimal use of local distributed generators

2) Feeding of local loads;

3) Reducing the operating cost;

4) Detection of islanding;

5) Synchronization of microgrid with the utility grid;

Important research has been conducted in the area of Microgrids, which may take many different sizes and forms [7]-[11]. Communication infrastructure operating between the power sources, to solve the optimization problem for/of voltage and frequencies, have been proposed and a rational method of building Microgrids optimized for cost and subject to reliability constraints have been presented.

1.4. Objectives and Contributions of Thesis

The main objective of this thesis is to develop a Microgrid model and simulate it under various conditions such as local generation, load mismatch, voltage and frequency control. These conditions are presented to be as close as possible to reality. The simulations are carried out using Matlab/Simulink. The basic advantage of using this software is that, there are readily available components in Simulink. The components used to build a microgrid can be modified or edited according to our needs. At first, a Microgrid model is formed and at a steady state, their transient responses when the inputs are changing are observed. Based on these, the model is developed to optimize the varying conditions. Meanwhile, it is intended that the models and results produced in this

thesis will form a baseline for further model development and ultimately lead to an ideal, if not closest to an ideal Microgrid. This long term goal is to have a highly sophisticated and complete model of a Microgrid.

1.5. Modeling of Microgrids

Analyzing a Microgrid requires suitable dynamic models for all the components forming the Microgrid. As the components utilized in the Microgrid model symbolize new potential resources of energy generation, the thesis develops models that describe their dynamic behavior [13] [14]. A simple and flexible model for islanding studies and power management purposes of the microgrid is developed. The microgrid components which have been studied are the photo-voltaic cells, the maximum power point tracker, DC-AC inverter modeling, load and utility grid.

1.6. Outline of the Thesis

The study and work performed in this thesis is organized as follows. The Chapter 1 provides introduction and background of Distributed generation units, Islanding phenomena, basic reason for developing the Microgrids and components utilized for developing one. The main focus of Chapter 2 is on a detailed description of each component utilized in building the model of Microgrid. The components used are the Photovoltaic cell, DC-DC boost, DC-AC inverter, controller, load and utility Grid. In Chapter 3, the modeling of the above mentioned components is presented with reasoning. Chapter 4 investigates the basic operation of the developed model to validate the operations of each component when they are coupled with each other. The end chapter 5 deals with conclusion and future scope of the work presented in thesis.

CHAPTER 2

MICROGRID COMPONENTS

2.1. Introduction

This chapter discusses the components used in developing a microgrid. For understanding the behavior of microgrid, each of these components is discussed in detail with their operations. The components described are a photo-voltaic cell, DC-DC booster, DC-AC inverter, programmable switch, passive load, load controller and utility grid. At the end, all the models are combined to form a complete model of microgrid and the whole operation is discussed theoretically.

2.2. Photovoltaic Cells

The photovoltaics (PVs) are always an attractive source of renewable energy for distributed power generation. The main advantage is their relatively small size and noiseless operation [1]-[4]. Applications of photovoltaics are significantly increasing all over the world as its potential is being observed. Photovoltaic generating technologies have the advantage that more units can be added to meet the load increase demand [10]. Apart from this, the main advantages of photovoltaics are:

(i) Short lead time to design, install and start up a new plant

(ii) Highly modular structure

(iii) Power output matches very well with peak load demands most often.

(iv) Static structure with no moving parts and therefore, no noise

(v) High power capability per unit of weight

(vi) Longer life with little maintenance

(vii) Highly mobile due to light weight.

Basically a solar cell as the name suggests, is a device that converts the energy of sunlight directly into electricity by the photovoltaic effect. That is one of the reasons it is called a Photovoltaic cell. A group of such individual photovoltaic cells bunched together can be called photovoltaic panels or photovoltaic modules or photovoltaic arrays.

Photovoltaic cells can be classified into four groups:

(i) Crystalline cells

(ii) Thin-film cells

(iii) Dye-sensitized solar cells

(iv) Multilayer cells.

Multilayer solar cells can also be considered as several layers of thin film Photovoltaic cells.

(i) Crystalline cells: These types of photovoltaic cells possess single junction devices. Crystalline cells are also termed as first generation photovoltaics. Therefore, at the initial stages of development, the production technology involved high energy and labor inputs which in turn resulted in avoiding any significant progress in reducing production costs [5]. A crystalline cell with single junction silicon devices being developed now is nearing the calculated efficiency of 24% and they reach the energy payback period of 5-7 years.

(ii) Thin film cells: High energy requirements and production costs of photovoltaic cells resulted in the development of thin film cells. The major materials used in thin film cells are Cadmium Telluride (CdTe), Copper Indium, Gallium Selenide, Amorphous Silicon [4]. Thin film cells also called

as Second generation of photovoltaic cells hold assurance of higher conversion rates with cheaper production costs.

(iii) Multilayer cells: Also called the third generation photovoltaic cells, the main aim was to improve the bad electrical performance of the second generation photovoltaic cells, while maintaining low production costs. The approaches in this technology are to use multi junction photovoltaic cells, concentration of the incident spectrum and thermal generation by Ultra-violet light to improve the voltage or carrier collection. With multilayer cells, the efficiency of photovoltaic cells is increasing the calculated theoretical efficiency.

At present, major research is being one worldwide on photovoltaic cells with the aim of increasing the efficiency, reducing the production costs.

2.2.1. Energy conversion efficiency of PV cell

The energy conversion efficiency (η) of a photo voltaic cell can be calculated as the percentage of power absorbed by the photo voltaic cell and converted to electric power when it is connected to an electrical circuit. It can also be termed as a ratio of maximum power point to the incident light irradiance [10].

$$\eta = \frac{P_m}{E\ X\ A_c}$$

Under standard test conditions, the specified temperature is 25 °C; irradiance is 1000 W/m^2, while the air mass is 1.5 spectrums. These conditions are usually observed during a clear day with sun and tilted at a 37^o tilted surface with sun at an angle of 41.81^o. Also these specified conditions are ideally met during noon of the day when the photo voltaic cell is directly underneath the sun.

The losses caused in a photovoltaic cell can be classified as reflectance losses, thermodynamic efficiency, recombination losses and resistive electrical loss. The total competence of a photovoltaic cell is the product of each of these above mentioned losses. As it is quite complex in measuring these parameters, other factors are taken into account such as thermodynamic efficiency, quantum efficiency, V_{oc} ratio and fill factor. While the reflectance losses come under quantum efficiency, recombination losses are classified under quantum efficiency, V_{oc} ratio and fill factor. The normal resistive losses are classified under fill factor and a part of quantum efficiency, V_{oc} ratio.

The effect of ambient irradiation G_a and the cell temperature T_c on the photo voltaic cell's behavior can be shown in the figure below:

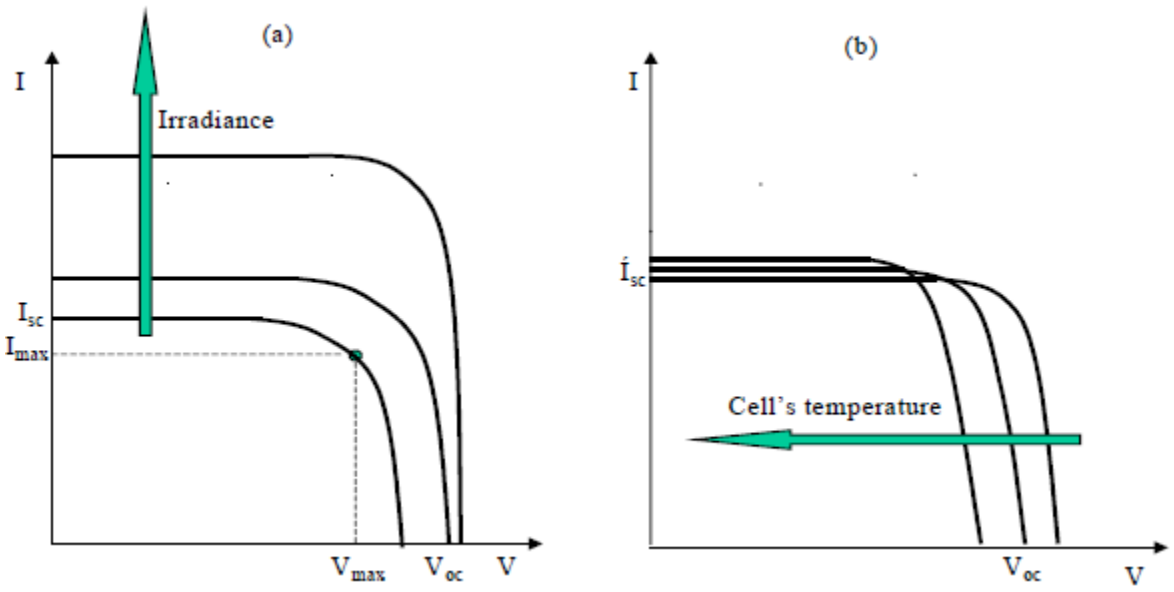

Fig 2.1 Influence of ambient irradiation on cell's temperature and cell characteristics.

In the above figure, we observe that the open circuit voltage increases in terms of log with the ambient irradiation, while the short circuit current is a linear function of the ambient irradiation. The arrow marks indicates the direction in which the irradiation and cell temperature respectively increase. Cell's temperature has an heavy influence on open circuit voltage, which is linear in effect with the photo voltaic cell's temperature. Therefore the photo voltaic cell tends to have a reduced efficiency. The short circuit current also contributes in the increase of cell temperature.

2.3. Maximum Power Point Tracker

A maximum power point tracker or MPPT can be termed as a highly efficient DC-DC converter. The main duty of maximum power point tracker is to track the maximum power point for the photovoltaic cell [12]. Maximum power point tracker converts the power to either a voltage or current which is necessary to be supplied to the connected load. Photovoltaic cells have a unique point of operation, where the current and voltage produced by the solar cell results in a maximum power output [19]. As per Ohm's law, the values of voltage and current at this point correspond to a particular resistance.

There is an exponential relation between current and voltage and the maximum power point takes place when the resistance is equal to the negative of the differential resistance. It is feasible to reach the power maximum power point by using some types of control circuit or logic.

From several MPPT techniques, perturb and observe [P&O] method has gained wide prominence. This is due to the fact that that P&O algorithm has a simple control structure with few measured parameters required for the power tracking. On top of this, the P&O technique doesn't depend on the photovoltaic module characteristics during the MPPT

and therefore can be utilized under any photovoltaic panel. As the name suggests, the technique operates by sporadically perturbing the control variable and comparing the instantaneous photovoltaic output power after perturbation with the value obtained before. This resultant value obtained from the comparison decides the direction of next perturbation.

The perturbation and observe technique when applied in MPPT technique plays an important role in determining the accuracy and speed at which the operating point moves. In a given perturbation interval, the larger the perturbation step, the faster the operating point can be driven to the MPP. But with larger step sizes, form larger intrinsic oscillations around the MPP in steady state which would reduce the photovoltaic power conversion rate. Likewise, a smaller perturbation reduces the magnitude of oscillation around the MPP and increases the energy conversion efficiency. But this can be achieved only under steady state and therefore under transient conditions, the MPP remains obscure. A varying step size may help overcome these problems.

Conventional DC-DC converter executes the maximum power point tracking for the whole photovoltaic array as a unity or single system. In such converters, the same current modeled by the converter flows through the entire photovoltaic panels in the strong. But with different panels having different IV curves, this results in below par performance and loss of energy. A novel method of avoiding this is by tracking the maximum power point for each panel individually [18], [19]. This way, each panel performs at its peak. Technologies like power optimizers are developed to maximize the energy production from the photovoltaic systems.

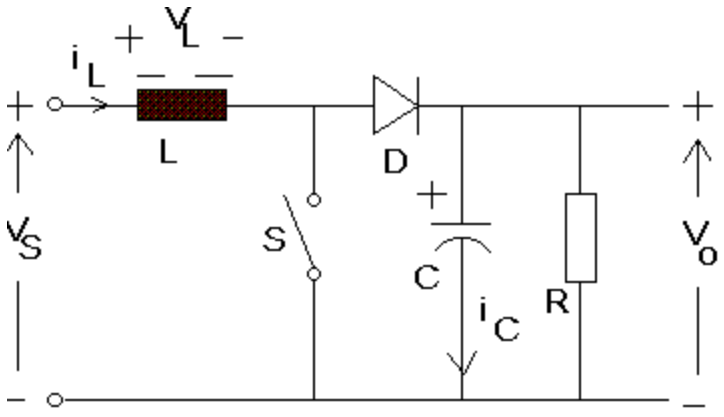

Fig 2.2 Basic Boost converter which is used as DC-DC boost.

In the circuit analysis of the boost converter, it can be noticed that the driving factor behind the circuit is the ability of inductor to resist changes in current. Therefore, when it is being charged, it behaves as a load absorbing some energy and while discharging it behaves as a source. It should be mentioned that the voltage produced by the inductor during its discharge phase is directly proportional to the change in the current.

When the switch S in the above figure is closed, it results in an increase of the inductor current and during OFF state i.e. when the switch is open, the energy is stored in the capacitor as the energy flows through the diode D, capacitor C and load R.

When the boost converter operates in a continuous mode, the current passing through the inductor stays above zero in all cases [21]-[23]. The output voltage can be calculated by considering a case of an ideal converter operating in steady conditions:

While in ON-state when the switch S is closed, the input voltage (V_i) appears across the inductor, which causes a change in current (I_L) flowing through the inductor during a time period (t) by the formula:

$$\frac{\Delta I_L}{\Delta t} = \frac{V_i}{L}$$

At the end of the On-state, the:

$$\Delta I_{LON} = \frac{1}{L}\int_0^{DT} V_i \, \partial t = \frac{DT}{L} V_i$$

Where, D is the duty cycle representing a part of commutation period T during which the switch is ON.

While in OFF-state, the switch S is open, so the inductor current flows through the load. If we consider zero voltage drops in the diode, and a capacitor large enough for its voltage to remain constant, the evolution of I_L is:

$$V_i - V_o = L\frac{dI_L}{dt}$$

The variation of I_L during the OFF-period:

$$\Delta I_{LOFF} = \int_0^{(1-D)T} \frac{(V_i - V_o)dt}{L} = \frac{(V_i - V_o)(1-D)T}{L}$$

Considering that the converter operates in steady-state conditions, the amount of energy stored in each of its components has to be the same at the beginning and at the end of each commutation cycle. In particular, the energy stored in the inductor is given by:

$$E = \frac{1}{2} L I_L^2$$

Therefore, the inductor current has to be the same at the beginning and the end of the commutation cycle.

$$\Delta I_{LON} + \Delta I_{LOFF} = 0$$

Substituting ΔI_{LON} and ΔI_{LOFF} by their expressions yields:

$$\Delta I_{LON} + \Delta I_{LOFF} = \frac{V_i DT}{L} + \frac{(V_i - V_o)(1-D)T}{L} = 0$$

This can be written as:

$$\frac{V_0}{V_i} = \frac{1}{1-D}$$

Therefore the Duty cycle can be calculated as:

$$D = 1 - \frac{V_i}{V_o}$$

From the above expression it can be observed that the output voltage is always higher than the input voltage and that it increases with D, theoretically to infinity as D approaches 1.

Therefore a Boost dc-dc converter can be utilized as a MPPT due to the fact that the output dc voltage from the converter is always greater than the input dc voltage. This is valid under all circumstances of the photovoltaic panel.

Grid tied photovoltaic inverters make use of maximum power point tracking system to maximize the power from a photovoltaic array and convert this into alternating current.

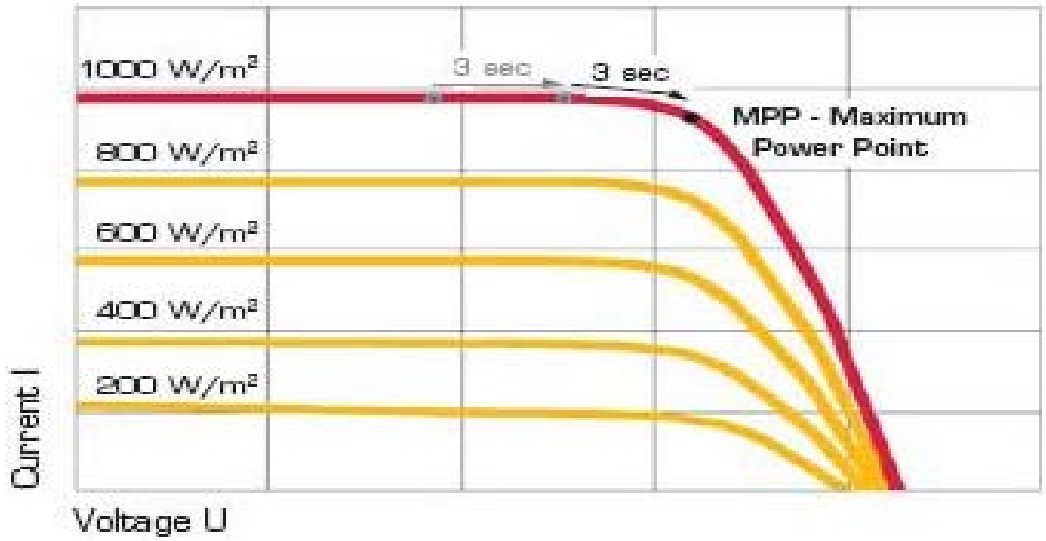

Fig 2.3 IV curve of MPPT

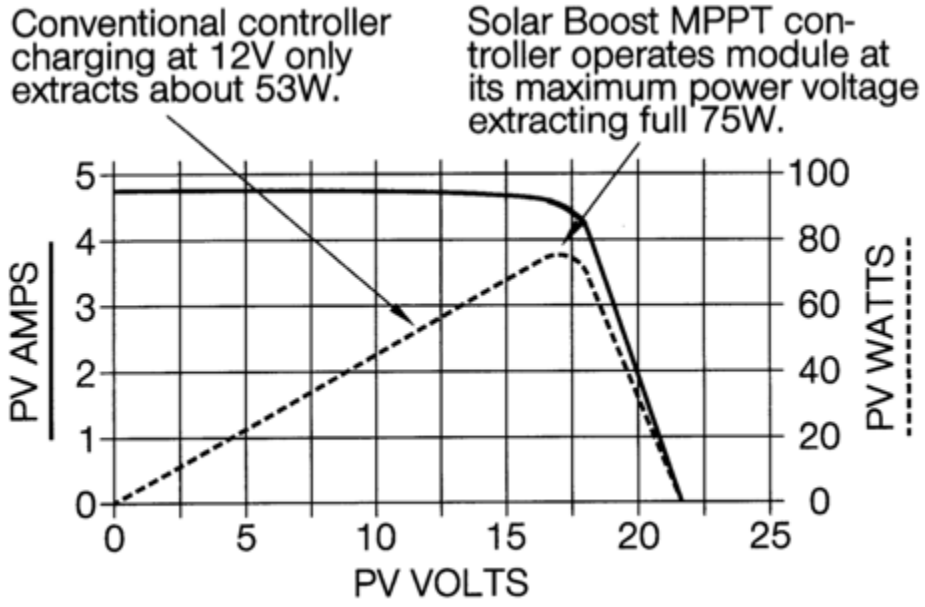

Fig 2.4 Typical 75W PV module current-voltage and power-voltage at standard test.

2.4. DC-AC Inverter

An inverter is required to convert the direct current (DC) to alternating current (AC). The direct current produced by the photovoltaic cells needs to be converted to an alternating current with appropriate amplitude and frequency in relative to the utility grid. This ensures the model to be a grid tie inverter [21]-[24].

A DC-AC inverter can be modeled using various fully controlled components such as IGBTs with anti parallel diodes, switches thyristor diodes etc and with the use of appropriate transformers and control circuits, the desired voltage and frequency can be obtained [13]. In this thesis, IGBTs have been used as switches for the inverter. There are several reasons for opting Insulate gate bipolar transistor [IGBT] as switch. The advantage of is that IGBT is a three terminal power semiconductor device known for high efficiency and fast switching. The basic model of IGBT diode is designed to swiftly turn ON and OFF.

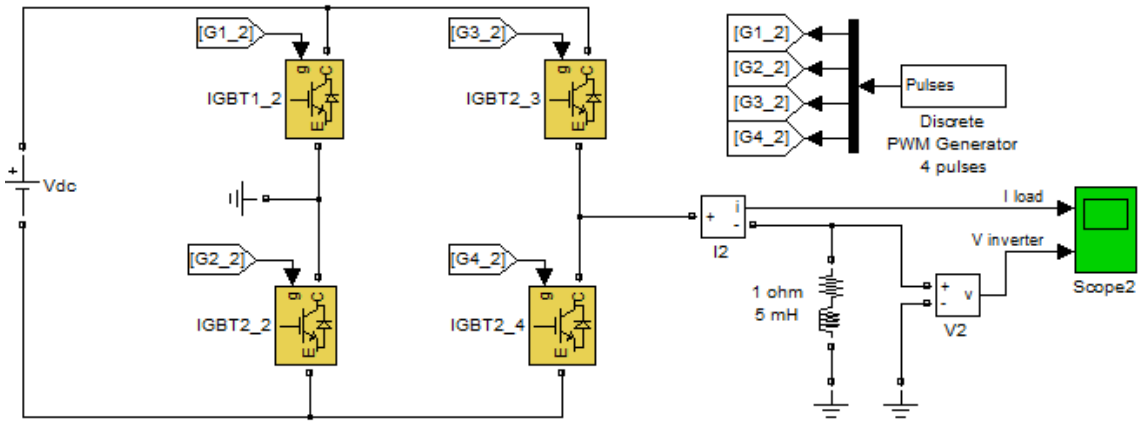

Fig 2.5 Full bridge IGBT inverter.

The inverter model consists of four IGBT diodes named individually as T1, T2, T3 and T4. This four-diode model bridge is fired pulses from a Pulse width generator. The pulses cause the alternate diodes T1 and T4 to turn ON while the diodes T2 and T3 remain OFF [13]-[16]. In the next sequence, diodes T2 and T3 are turned ON while the diodes T1 and T4 remain OFF. This alternating switching of diodes converts the input direct current to an alternating current.

The pulse width modulator is used to generate the firing pulses. Simulink provides a PWM block [13]. We have an option of modeling the pulse width generator with either an input modulating sinusoidal wave or an external sinusoidal wave. The PWM generator in thesis has been modeled to have an external sinusoidal wave. This helps in developing a grid-tie inverter.

The PWM Generator block generates pulses for carrier-based pulse width modulation [PWM] converters using two-level topology. The block can be used to fire the forced-commutated devices [IGBTs] of single-phase bridges.

The pulses are generated by comparing a triangular carrier waveform to a reference modulating signal. The modulating signals can be generated by the PWM generator itself, or they can be a vector of external signals connected at the input of the block [12]-[18]. One reference signal is needed to generate the pulses for a single- or a two-arm bridge, and three reference signals are needed to generate the pulses for a three-phase, single or double bridge.

The amplitude [modulation], phase, and frequency of the reference signals are set to control the output voltage (on the AC terminals) of the bridge connected to the PWM Generator block. The two pulses firing the two devices of a given arm bridge are

complementary. For example, pulse 4 is low [0] when pulse 3 is high [1]. The two pulses firing the two devices of a given arm bridge are complementary. For example, pulse 4 is low [0] when pulse 3 is high [1]. This is illustrated in the next two figures. The following figure displays the two pulses generated by the PWM Generator block when it is programmed to control a single phase full bridge IGBT converter.

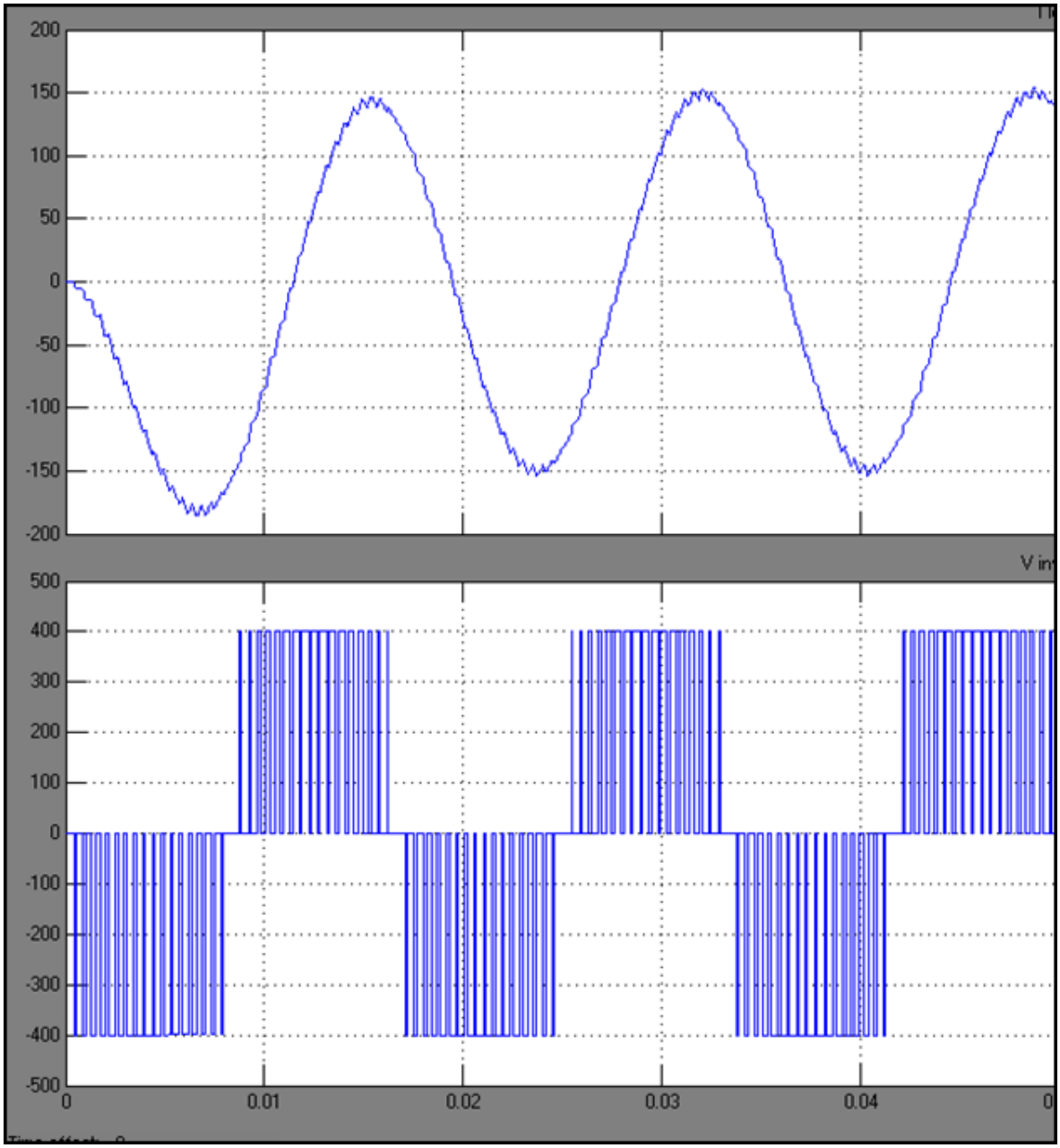

Figure2.6 Waveform of a single phase full bridge Inverter

The triangular carrier signal is compared with the sinusoidal modulating signal. When the modulating signal is greater than the carrier pulse 1 is high [1] and pulse 2 is low [0].

For a single-phase two-arm bridge the modulating signal used for arm 2 is the negative of modulating signal used for arm 1 [180 degrees phase shift].

Once the direct current is converted to an alternating current, the output from the inverter is a pulse width modulated wave with amplitude that is proportional to the input direct current. It is necessary to convert this square wave to a sinusoidal wave with appropriate frequency. A low pass filter with and inductor [L] and capacitor [C] is used for this transformation [21]. As the name suggests, a low pass filter is a filter that allows low frequency signals, but attenuates or reduces the amplitude of high frequency signals or signals that are above the cut off frequency such that it is either completely absent or is present in a negligible amount.

$$\frac{V_o}{V_L} = \frac{\frac{1}{jW_c}}{\frac{1}{jW_c} + jW_c} = \left|\frac{1}{1-W^2\,L_c}\right| V_i \qquad (1)$$

$$\frac{1}{1-W^2\,L^C} = \frac{-1}{\sqrt{2}} \qquad (2)$$

$$1 - W^2\,LC = -\sqrt{2} \qquad (3)$$

$$W^2 LC = \frac{1+\sqrt{2}}{L\,C} \qquad (4)$$

$$W^* = W^0\left(\frac{1+\sqrt{2}}{L\,C}\right) \qquad (5)$$

The cut of frequency of the low pass filter is calculated using the values of the inductor and capacitor. An ideal low pass filter completely attenuates the frequencies above the cutoff frequency, while allowing the transmission of signals with lesser frequency [22]. Though it is possible to realize an ideal low pass filter mathematically by having the signal multiplied by a rectangular function in frequency domain, it is very difficult to realize in practice and therefore needs to be approximated to a certain extent [23]. Low pass filters for real time applications are approximated as an ideal filter by trimming the infinite impulse response in order to develop a finite impulse response.

The obtained sinusoidal wave is then supplied to the one side of load while the other side of the load is connected to the utility grid. This forms a basic complete model of grid connected photo-voltaic panel.

2.5. Load

A load voltage characteristic is an expression which gives an active power or reactive power consumed by the load as a function of voltage [28]. It is also an independent variable which we name the load demand.

Considering z as a general form of load characteristic:

$$P = P(z, V) \qquad (1)$$

$$Q = Q(z, V) \qquad (2)$$

It is crucial to signify the clear difference between the real consumed load power (P,Q) and the load demand z [24] [28]. This is required to understand the basic instability mechanism by which the increased demand may result in reduced consumption power.

2.5.1. Exponential load

The most prominently used load characteristic is called the exponential load which can be presented as:

$$P = zP_0\left(\frac{V}{V_0}\right)^{\alpha} \qquad (3)$$

$$Q = zQ_0\left(\frac{V}{V_0}\right)^{\beta} \qquad (4)$$

Where z is the dimensionless demand variable, $V_0$is the reference voltage and exponents α and β depend on the type of load such as motor, heating, lighting etc. It should be made aware that zP_0 and $zQ_0$are the active and reactive powers consumed by the load under a voltage V equal to the reference V_0 and relate to the amount of connected equipment. These can also be called the nominal load powers in contrast to the consumed powers P, Q.

The following table presents three cases of load exponents:

Load Component	α	β
Incandescent lamps	1.54	-
Room air conditioner	0.50	2.5
Furnace fan	0.08	1.6
Battery charger	2.59	4.06
Electronic compact fluorescent	0.95-1.03	0.31-0.46
Conventional fluorescent	2.07	3.21

Table 2.1: Sample of fractional load exponents

$\alpha = \beta = 2$: Constant impendence load (Z)

$\alpha = \beta = 1$: Constant current load (I)

$\alpha = \beta = 0$: Constant power load (P)

It is important to note that while using exponential load at low voltage levels, when voltage drops below a threshold value, many loads may be disconnected. If not, the characteristics of these loads will be completely altered.

Assuming Z=1, due to exponential relation, the reference voltage V_0 and the corresponding P_o, Q_o can be specified arbitrarily without changing the characteristic. Consider the instance a voltage level V_1, for which the load power is

$$P_1 = P_0 \left(\frac{V_1}{V_0}\right)^{\alpha} \quad (5)$$

By using the above relation to substitute $P_{o,}$ in equation 3 we get:

$$P = P_1 \left(\frac{V}{V_1}\right)^{\alpha} \quad (6)$$

Therefore we have replaced V_0 with V_1 and P_o with P_1 showing that any voltage level can be used as a reference, in order to initialize the exponential model.

The exponents α and β of the exponential load model determine the sensitivity of the load power to voltage [24]. Assuming any reference voltage V_0, for which the load active power is P_0, the sensitivity of active power with respect to voltage is calculated as:

$$\frac{dP}{dV} = \alpha P_0 \left(\frac{V}{V_0}\right)^{\alpha-1} \frac{1}{V_0} \quad (7)$$

A similar relation holds good for reactive power. By rearranging the above equations and evaluating by the sensitivity at $V=V_o$ we find:

$$\frac{\frac{dP}{P_0}}{\frac{dV}{V_0}} = \alpha \quad (8)$$

$$\frac{\frac{dQ}{Q_0}}{\frac{dV}{V_0}} = \beta \quad (9)$$

Therefore, the normalized sensitivities of real and reactive load power are equal to the corresponding load exponents.

2.5.2. Polynomial load

From the above table, different load components exhibit different voltage characteristics. Therefore an alternative load representation based on summing up load components which have the same exponent [24]. When the exponents are all integer, the load characteristic becomes polynomial in V. A special case worth mentioning is the ZIP model, which is made up of three components: constant impendence, constant current and constant power. The real and reactive characteristics of ZIP load model are given by the following quadratic expressions:

$$P = zP_0 \left[a_p \left(\frac{V}{V_0} \right)^2 + b_p \frac{V}{V_0} + c_p \right] \quad (10)$$

$$Q = zQ_0 \left[a_Q \left(\frac{V}{V_0} \right)^2 + b_{pQ} \frac{V}{V_0} + c_Q \right] \quad (11)$$

Where $a_p+b_p+c_p= a_q+b_q+c_q=1$, while zP_0 and $zQ_0$are the load real and reactive powers consumed at the reference voltage V_o.

When the polynomial load parameters are obtained from measurements, some of them usually the one defining the current contribution b_p may assume negative values.

2.5.3. Load restoration dynamics

The power consumption by the load depends on their voltage characteristics. This dependency may be permanent if the load is purely static or it may change with time if the load is dynamic [24] [28]. The dynamics of various load components and control mechanisms tend to restore load power at least to a certain extent. We can name it as load restoration.

While considering the specific loads, a concise way to describe load dynamics in general is presented. Consider the power consumed by the load at any time depends on the instantaneous value of the load state variable, denoted as x:

$$P = P_t(z, V, x) \quad (12)$$

$$Q = Q_t(z, V, x) \quad (13)$$

Where P_t and Q_t are smooth functions of demand, voltage and load state and are called the transient load characteristics [28]. Also consider the load dynamics are described by the smooth differential equation:

$$x = f(z, V, x) \quad (14)$$

The steady state of load dynamics is characterized by the following algebraic expression:

$$f(z, V, x) = 0 \quad (15)$$

In general, equation 15 can be used to obtain the state variable x as function of z and V:

$$x = h(z, V) \quad (16)$$

With h satisfying:

$$f\big(z, V, h(z, V)\big) = 0 \quad (17)$$

Substituting equation 16 into 12 and 13, we get:

$$P = P_t\big(z, V, h(z, V)\big) = P_s(z, V) \quad (18)$$

$$Q = Q_t\big(z, V, h(z, V)\big) = Q_s(z, V) \quad (19)$$

Where P_s and Q_s are the steady state load characteristics [28]. Also the steady state load characteristics do not depend on the load state variable. The transition towards the steady state load characteristics is driven by the load dynamics.

Usually the transient load characteristic is more sensitive to voltage than the steady state load characteristic, so that in the steady state, the load power is restored closer to its pre-disturbance value [28]. A typical example is the transition from constant impedance to constant power load.

In this thesis, a parallel Resistive (R) and Inductive (L) load is used to draw the power from a photovoltaic panel and utility grid. It acts as passive load. It is modeled such that it remains connected to the photovoltaic panel throughout the simulation, while the connection to the utility grid can be programmed using a circuit breaker. In this thesis, the load is programmed with values such that the amount of active power and reactive power consumed by the load accounts to the sum of the active powers and reactive powers being supplied individually by a photovoltaic panel and the utility grid.

2.6. Utility Grid

Utility grid or the main supply is connected to one side of the load. In this thesis, we use an alternating current (AC) voltage supply which acts as a utility grid. The values specified for this voltage supply corresponds with the voltage across the photovoltaic terminal.

2.7. Synchronization

To keep the inverter always in synchronization with the load and the utility grid, a linear transformer is used to feed back a part of voltage being supplied by the inverter back to the pulse width modulator. The pulse width modulator is designed to modulate the voltage at a frequency which is a multiple of 60 Hz. But the utility grid supplies AC voltage at frequency of 60 Hz. Also the amplitude of the carrier wave in the pulse width modulator is 1 V while that of AC supply is 170 V. To synchronize the dc- side with the utility, a linear transformer with two winding ratio of 170:1 is used to feed back the voltage back to the pulse width modulator. This way, the voltage of the inverter is kept in phase with that of utility grid.

CHAPTER 3

Modeling of Microgrid

3.1. Introduction

In this chapter, the modeling of the components which were used while building the electrical model for this thesis will be discussed. The photovoltaic panel, maximum power point tracking system, DC-AC inverter circuit, low pass filter, load, utility grid and the power electronics interface which were assembled as individual components and later coupled together to form a grid connected distributed generation system, will be described in detail.

3.2. Photovoltaic Panel

It is well known that a photovoltaic array consists of a collection of solar cells which are connected in series and/or parallel. Each of these cells is basically a p-n diode which converts the incident light energy into electrical energy. The most widely used photovoltaic cell is a one diode model [1]-[4]. But in the cases where, the photo voltaic panel is supplied with an external supply of large voltage, it starts generating a current. This called is called the diode current of dark current and is named $I_{D.}$

The one-diode equivalent electrical model of the photo voltaic cell consists of a current supply I_L series with a resistance R_s and a parallel diode D and parallel resistance $R_{sh.}$

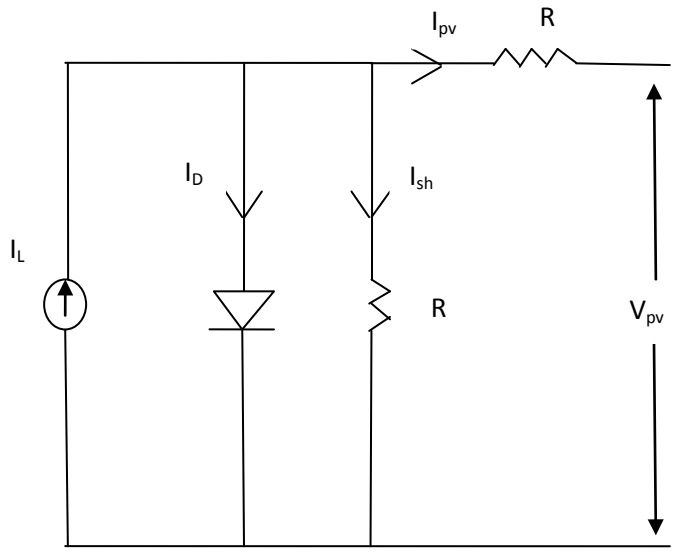

Figure 3.1 One diode equivalent model of photo-voltaic panel.

The resultant net current is the difference between the photocurrent I_{pv} and the normal current $I_{D.}$

$$I_{pv} = I_L - I_O = I_L - I_O \left(\exp\left(\frac{V_{PV} + I_{PV} R_S}{\alpha}\right) - 1\right)$$

In the above equation,

(i) I_L is light current.

(ii) I_0 is saturation current.

(iii) R_s is series resistance.

(iv) α = Thermal voltage timing completion factor.

The non-linear curves of $V_{pv} – I_{pv}$ and P-V_{pv} are as shown in the below graph:

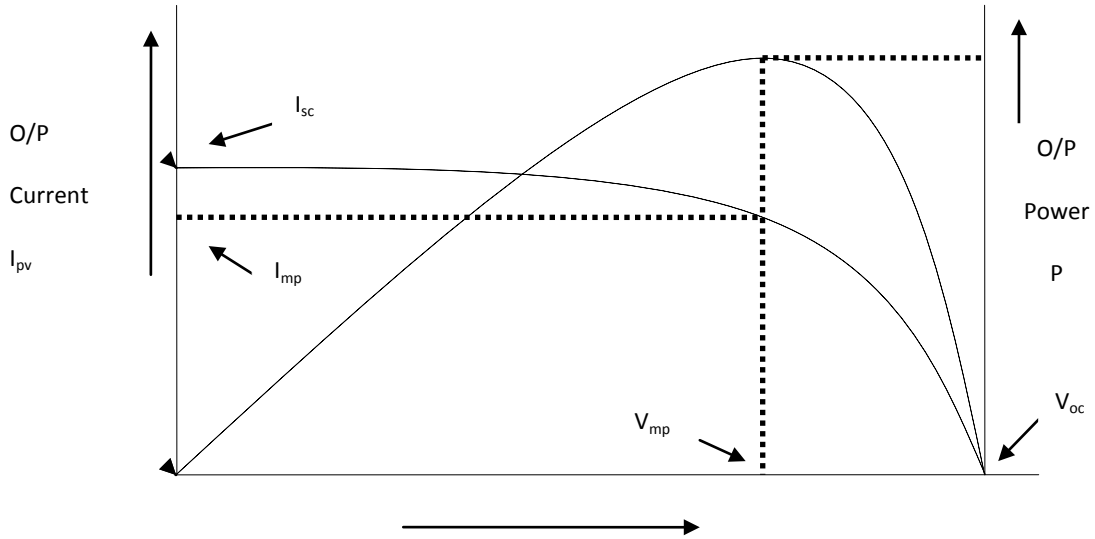

Figure 3.2 Current-Power of PV as a factor of V_{pu} voltage.

The above model can also be termed as a four parameter model. The equation for determining the four parameters are [3]:

1. Light current [I_L]:

$$I_L = \frac{G}{G_{ref}}(IL_{ref} + \mu_{ISC}(T_C - T_{Cref}))$$

In the above equation,

(i) G = solar irradiance (W/m^2);

(ii) G_{ref} = reference irradiance;

(iii) I_{Lref}= light current at the reference condition;

(iv) T_c= PV cell temperature (^oC);

(v) T_{Cref}=reference cell temperature;

(vi) μ_{Isc} = temperature coefficient of the short circuit current (A/^{o}C);

From the equation for light current, it can be observed that I_L is a function of both temperature and irradiance.

2. Saturation Current [I_o]:

$$I_O = I_{Oref}\left(\frac{T_{Cref} + 273}{T_C + 273}\right)^2 exp\left(\frac{e_{gap}\, q}{N_s \alpha_{ref}}\left(1 - \frac{T_{cref} + 273}{T_c + 273}\right)\right)$$

In the above equation,

(i) I_{oref} = saturation current at the reference condition (Amps);

(ii) e_{gap} = band gap of the material and is equal to 1.17 eV for Si materials;

(iii) N_s = number of cells in series of a photo voltaic module;

(iv) q = charge of an electron;

(v) α_{ref} = value of α at reference condition;

(vi) $I = I_{Lref} \exp\left(-\frac{V_{Ocref}}{\alpha_{ref}}\right)$

V_{ocref} = open circuit voltage of the photo voltaic module at reference condition (V).

3.2.1. Model of PV module

Cells are normally grouped into “modules”, which are encapsulated with various materials to protect the cells and the electrical connectors from the environment [2]. The manufacturers supply PV cells in modules, consisting of N_{PM} parallel branches, each with N_{SM} solar cells in series.

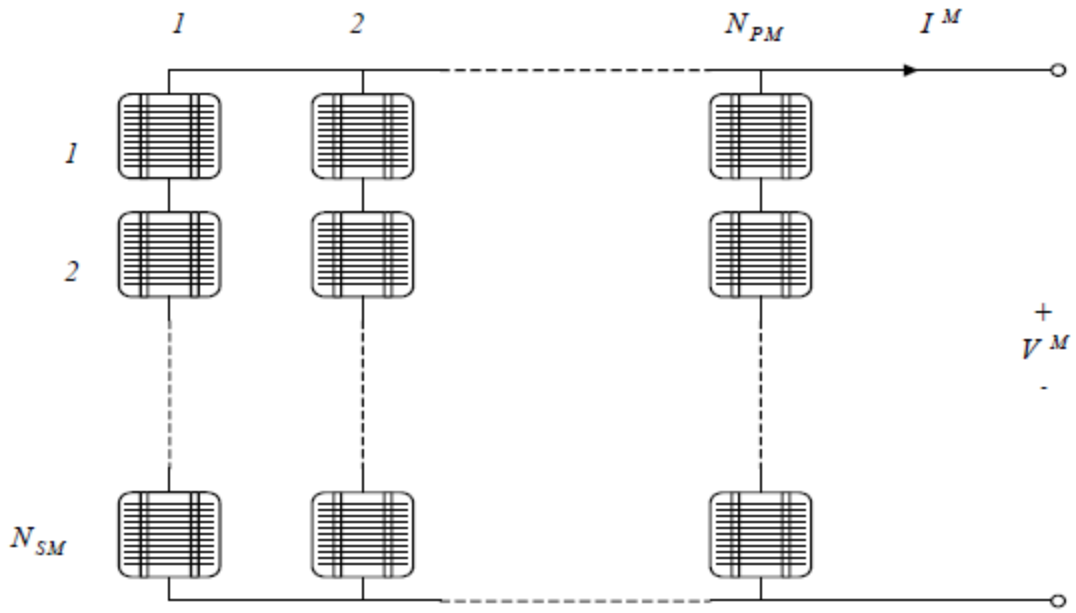

Figure 3.3 The photo voltaic module consisting of N_{PM} parallel branches, each of N_{SM} solar cells in series.

In order to have a clear specification of which element (cell or module) the parameters in the mathematical model are regarding, the following notation is used from now on: the parameters with superscript "*M* " are referring to the PV module, while the parameters with superscript "*C* " are referring to the solar cell. Thus, the applied voltage at the module's terminals is denoted by V^M, while the total generated current by the module is denoted by I^M.

A model for the PV module is obtained by replacing each cell in the above figure, by the equivalent diagram from basic electrical circuit. In the following, the mathematical model of a PV module is briefly reviewed. The advantage of this model is that it can be established applying only standard manufacturer supplied data for the modules and cells.

The PV module's current I^M under arbitrary operating conditions can thus be described as:

$$I^M = I_{SC}^M \left[1 - exp\left(\frac{V^M - V_{OC}^M + R_S^M . I^M}{N_{SM} V_t^c}\right)\right]$$

The expression of the photo voltaic module's current I^M is an implicit function, being dependent on:

- The short circuit current of the module, which is $I_{SC}^M = N_{PM} . I_{SC}^C$
- The open circuit voltage of the module, which is $V_{OC}^M = N_{SM} . V_{OC}^C$
- The equivalent serial resistance of the module, which is $R_S^M = [N_{SM}/N_{PM}] . R_S^C$
- The thermal voltage in the p-n diode of the photo voltaic solar cell, which is $V_t^C = [mkT^C] / e$

3.3. DC-AC inverter

The inverter is characterized by a power dependent efficiency η. The role of the inverter is to keep on the AC side the voltage constant at the rated voltage which is 170V and to convert the input power P_{in} into the output power P_{out} with the best possible efficiency. The efficiency of the inverter is thus modeled as:

$$\eta = \frac{P_{out}}{P_{in}} = \frac{V_{ac} I_{ac} \cos \emptyset}{V_{dc} I_{dc}} \Rightarrow I_{dc} = \frac{V_{ac} I_{ac} \cos \emptyset}{\mu V_{dc}}$$

Where I_{dc} is the current required by the inverter from the DC side (for example, from the controller) in order to be able to keep the rated voltage on the AC side (for example on the load). V_{dc} is the input voltage for the inverter delivered by the DC side, for example by the controller.

The efficiency of the inverter is defined as:

$$\eta = \frac{P_{out}}{P_{in}} = \frac{P_{ac}}{P_{dc}} = \frac{P_{ac}}{V_{dc} I_{dc}}$$

Where P_{AC} is the measured power on the AC-side of the inverter, while P_{DC} is the power on the DC-side of the inverter. The DC-voltage is $V_{DC} = V_{load}$, while the DC-current is $I_{dc} = I_{load}$.

The inverter has only two operating modes (load or not), which can be switched by an"on-off" button. In order to estimate the efficiency of the inverter, it is necessary to expose the system to different loads and therefore to perform the measurements on the inverter using a variable load. It should be mentioned that in the determination of the inverter efficiency, the constant load is completely disconnected and a variable load c is applied. In each step, P_{ac}, V_{load} and I_{load} are measured.

In this thesis, Matlab/Simulink provides a universal bridge inverter. This component can be modeled to implement a universal three phase power converter which consists of six power switches. The desirable power switch and converter configuration can be chosen from the dialog box.

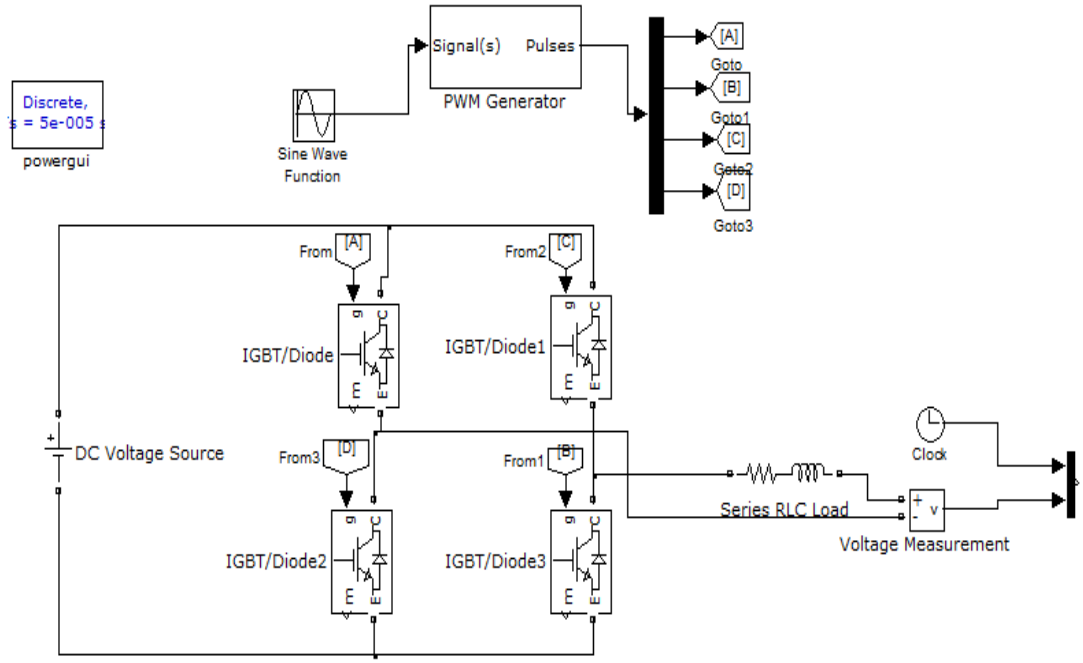

Figure 3.4 IGBT diode inverter (DC-AC)

The Universal Bridge block allows simulation of converters using both naturally commutated (line-commutated) power electronic devices (diodes or thyristors) and forced-commutated devices (GTO, IGBT, MOSFET).

The Universal Bridge block is the basic block for building two-level voltage-sourced converters (VSC). The device numbering is different if the power electronic devices are naturally commutated or forced-commutated.

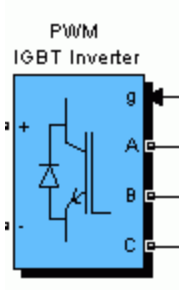

Figure 3.5 A PWM IGBT inverter

The following are the modeling factors of the DC-AC inverter circuit:

(i) Number of bridge arms

Set to 1 or 2 to get a single-phase converter (two or four switching devices). Set to 3 to get a three-phase converter connected in Graetz bridge configuration (six switching devices).

(ii) Snubber resistance Rs

The snubber resistance is represented in ohms (Ω). Set the Snubber resistance Rs parameter to infinity to eliminate the snubbers from the model.

(iii) Snubber capacitance Cs

The snubber capacitance, in farads (F). Set the Snubber capacitance Cs parameter to 0 to eliminate the snubbers, or to infinity to get a resistive snubber.

In order to avoid numerical oscillations when your system is discretized, you need to specify Rs and Cs snubber values for diode and thyristor bridges. For forced-commutated

devices (GTO, IGBT, or MOSFET), the bridge operates satisfactorily with purely resistive snubbers as long as firing pulses are sent to switching devices.

If firing pulses to forced-commutated devices are blocked, only anti parallel diodes operate, and the bridge operates as a diode rectifier. In this condition appropriate values of Rs and Cs must also be used.

When the system is discretized, use the following formulas to compute approximate values of Rs and Cs:

$$R_s > 2[T_s/C_s]$$

$$C_s < P_n/[1000.2\pi f.\ V_n^2]$$

Where, P_n = Nominal power of single or three phase converter (VA)

V_n = Nominal line to line AC voltage (V_{rms})

f = Fundamental frequency

T_s = Sample time

These Rs and Cs values are derived from the following two criteria:

- The snubber leakage current at fundamental frequency is less than 0.1% of nominal current when power electronic devices are not conducting.
- The RC time constant of snubbers is higher than two times the sample time Ts.

These Rs and Cs values that guarantee numerical stability of the discretized bridge can be different from actual values used in a physical circuit.

In this thesis, the universal bridge has been modeled as a full bridge, two arm IGBT inverter. The pulse width modulator fires the pulses for switching. The pulse width modulator in turn has an external supply connected to the sinusoidal carrier wave.

The reason for this ratio is due to the fact that, the amplitude of the triangle wave form in pulse width modulator is kept 1 and amplitude of the carrier wave is also kept 1. Therefore,

$m_a = 1$.

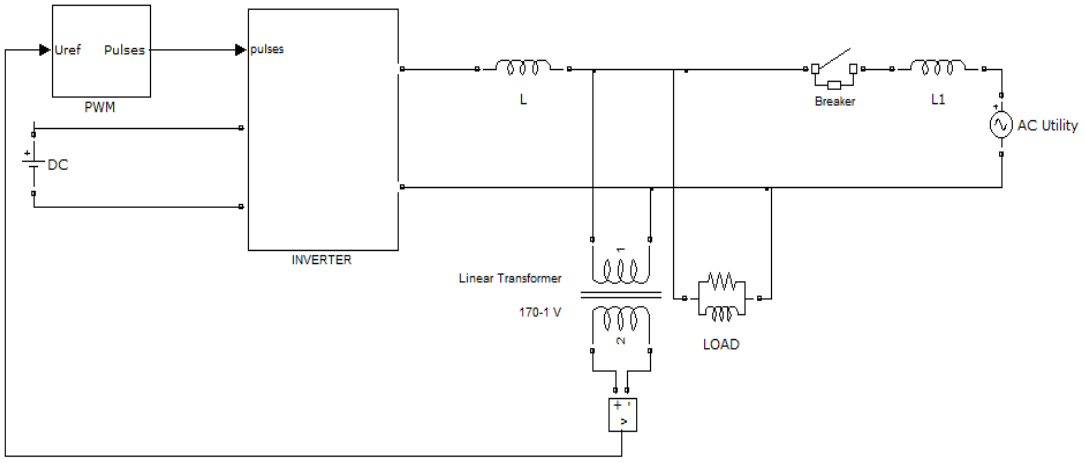

Figure 3.6 Schematic diagram of a grid tied inverter with load.

The utility grid supplies a voltage of 170 V peak. Therefore, it is necessary to tune the 170V to 1 V before feed it back again to the pulse width generator. This way, the inverter behaves as grid tie inverter.

The units such as voltage measurement and current measurement will be used to determine the current, voltage to be measured across, the photo voltaic terminal, utility terminal and also the load.

3.4. Load

The load is necessarily an electrical component which can draw a certain amount of power from the supply grid. The load used in thesis is a passive load. A passive load is used to keep overall electrical grid simple and therefore it would be easy to obtain the

voltage, current, real and reactive power waveform easily. The amount of power to be withdrawn is specified by modeling the load. Matlab/ Simulink provide a variety of loads. In this thesis, a parallel Resistive (R), Inductive (L) load has been utilized. A parallel RL load in Matlab/simulink

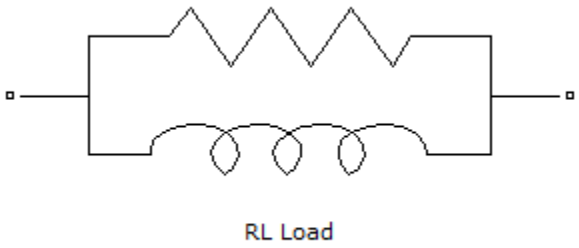

Figure 3.7 Parallel Resistive (R) and Inductive (L) load.

3.5. Utility Supply

The utility supply is nothing but a Alternating Current (AC) supply. Matlab/ Simulink allow a direct and simple component of AC voltage supply. The voltage peak specified for the utility grid is 170 V amplitude.

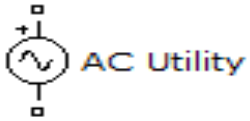

Figure 3.8 Alternating Current Utility.

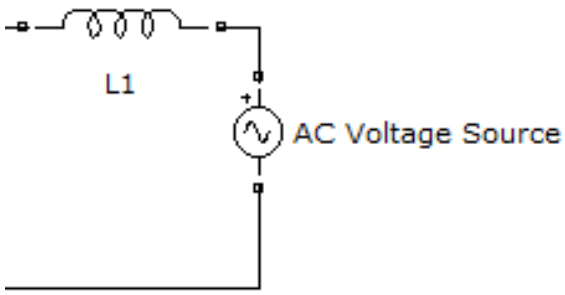

Figure 3.9 AC voltage connected to a thevenin inductance L1.

From the above figure, while the amplitude is 170 peak, it corresponds with the peak voltage obtained from the photo voltaic system which is again 170V. This way, the electrical system is in sync with each other. The thevenin inductor L1 = 0.000065.

CHAPTER 4

Simulation Results

4.1. Introduction

In this chapter, the microgrid model which was developed in the thesis will be simulated and results are posted. Initially, each individual component will be mentioned and the resultant waveform obtained from the respective module will be presented. Later, at the end, the whole micro grid, as a single entity will be mentioned in brief and the obtained results will be published. This way, it would be easy to configure the required parameters individually before connecting the entire grid. Thus, there would be a minimum probability of error in designing the electrical grid.

4.2. Stand Alone No-Load inverter

The photo voltaic panel is electrically transformed into a DC voltage supply. The direct current is supplied to the IGBT inverter. This inverter is fired with pulses from a Pulse width generator enables to alternatively switch two of its diodes at every single instant, thereby converting the direct current to an alternating current. An equivalent circuit representing the photo voltaic panel which is connected to the Inverter is as shown in figure below:

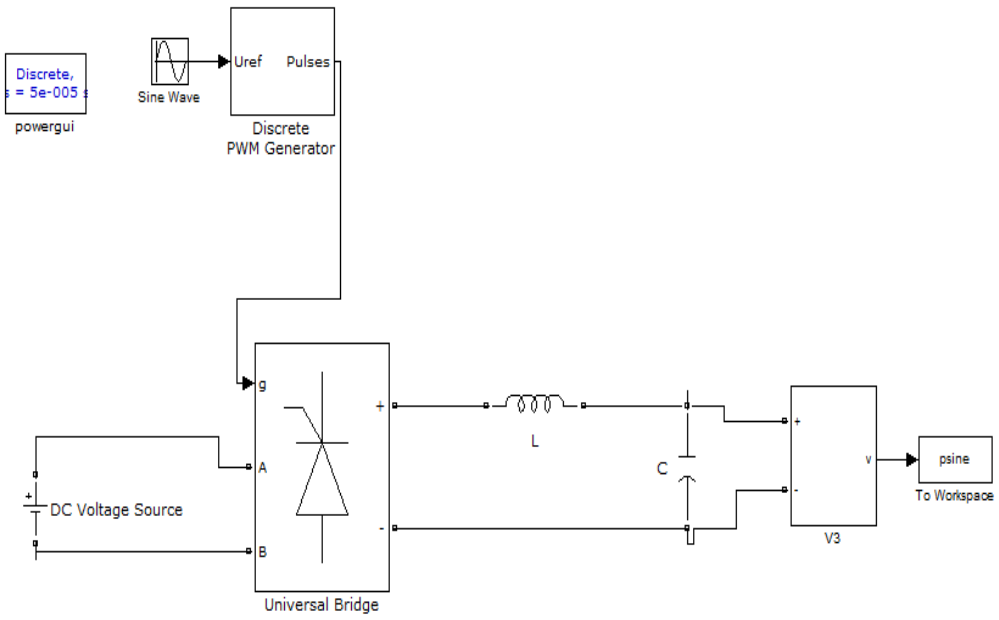

Figure 4.1 Electrical model of DC voltage source connected to an Inverter.

From the above figure it can be deduced that photovoltaic panel is replaced with a simplified DC voltage source. Universal bridge consists of IGBTs which perform the inverter functions. A discrete PWM generator is used to fire the pulses.

The amplitudes of both the modulating signal and the carrier signal is kept the same to maintain the m_a= 1.

A low pass filter is used to maintain the frequency of the inverter voltage to 60 Hz. A series inductor [L] and a parallel [C] is used to attenuate any frequency above 60 Hz. The designing of this filter can be explained with the following equations:

$$f_c = \frac{1}{2\pi\tau} = \frac{1}{2\pi RC}$$

$$\omega_c = \frac{1}{\tau} = \frac{1}{RC}$$

The values of the inductor and capacitor are modeled such that the cut off frequency f_c is 60 Hz.

The resultant waveform for the above circuit is as shown below.

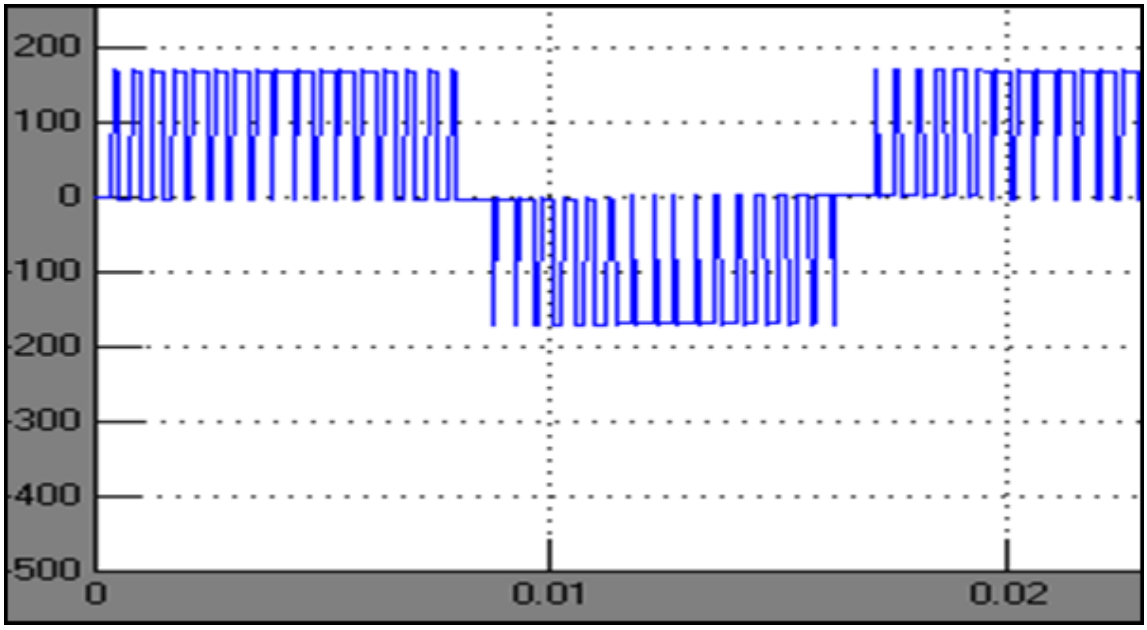

Figure 4.2: Square wave from the inverter before the filter LC circuit.

As seen in the above circuit, the inverter successfully converted the input direct current which is supplied by a DC source into an AC voltage. The inverter initially produces a PWM wave which develops due to the uni polar switching of the IGBT diodes of inverter.

The pulse width modulator uses the carrier frequency which is an odd value of 60 Hz. Therefore, it is very essential to attenuate such a high frequency especially when the voltage is being supplied to the load and utility grid. The utility grid having a frequency

of 60 Hz, it is only feasible to allow signals with frequency up to 60 Hz and eliminate any higher frequencies.

This is achieved in using a low pass filter. As mentioned in previous chapters, a low pass filter attenuates signals with frequency above the cut-off frequency, the filter in the thesis is modeled such that, the cut off frequency is 60 Hz. We use an inductive (L) and capacitive (C) filter to achieve this. While the inductor (L) is connected in series, the capacitor (C) is connected in parallel to the inverter. The values of the filter components were L = 0.00025 H and C = 0.000053 F. From the sinusoidal wave, we can observe that the resultant waveform has been successfully tuned to 60Hz.

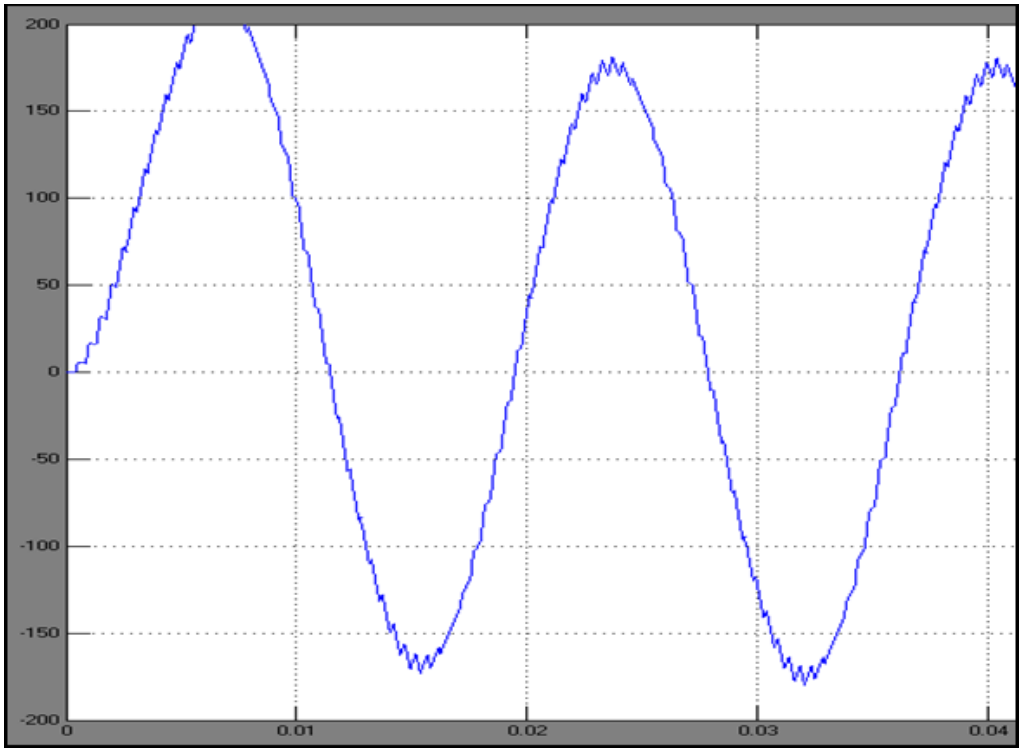

Figure4.3: A sinusoidal waveform obtained from the Low pass LC filter.

Similarly the active power and reactive power supplied by the inverter is calculated. This is a key step in order to achieve the right calculation being absorbed by the load. Ideally, both the photo voltaic module and the utility grid should split the load power depending on the load specifications.

In first case, a RL load is connected only to the inverter and an active power [P] and reactive power [Q] is observed. The circuit diagram with the load attached to the DC-AC inverter is shown below and the active power and reactive power consumed by the load is displayed.

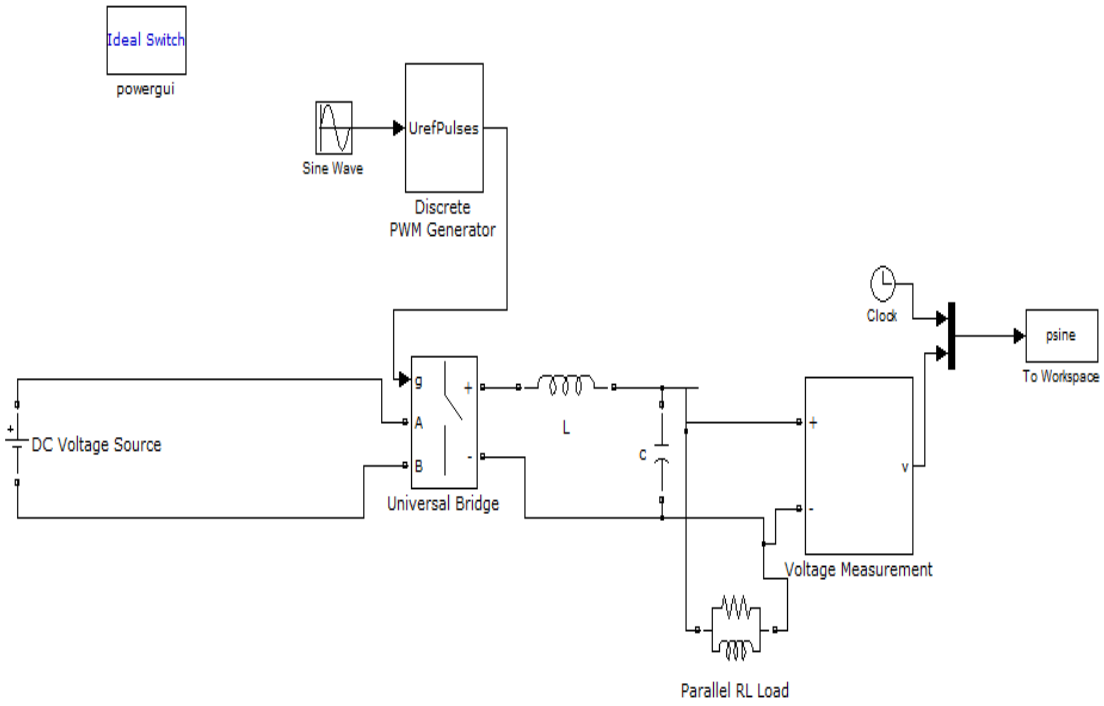

Figure 4.4. Parallel RL load connected to a stand-alone inverter.

The active power and reactive power supplied by the DC system was a smooth wave as show below. The DC voltage source generates the active power [P] and reactive power [Q] demanded by the parallel resistive [R] inductive [L] load. The load is specified that

the active power of the load [P_L] = 7000 W and the reactive power [Q_L] = 4000 Vars. Therefore observing the graph below shows us that, the inverter has been modeled to generate a right amount of active power and reactive power as demanded by the load.

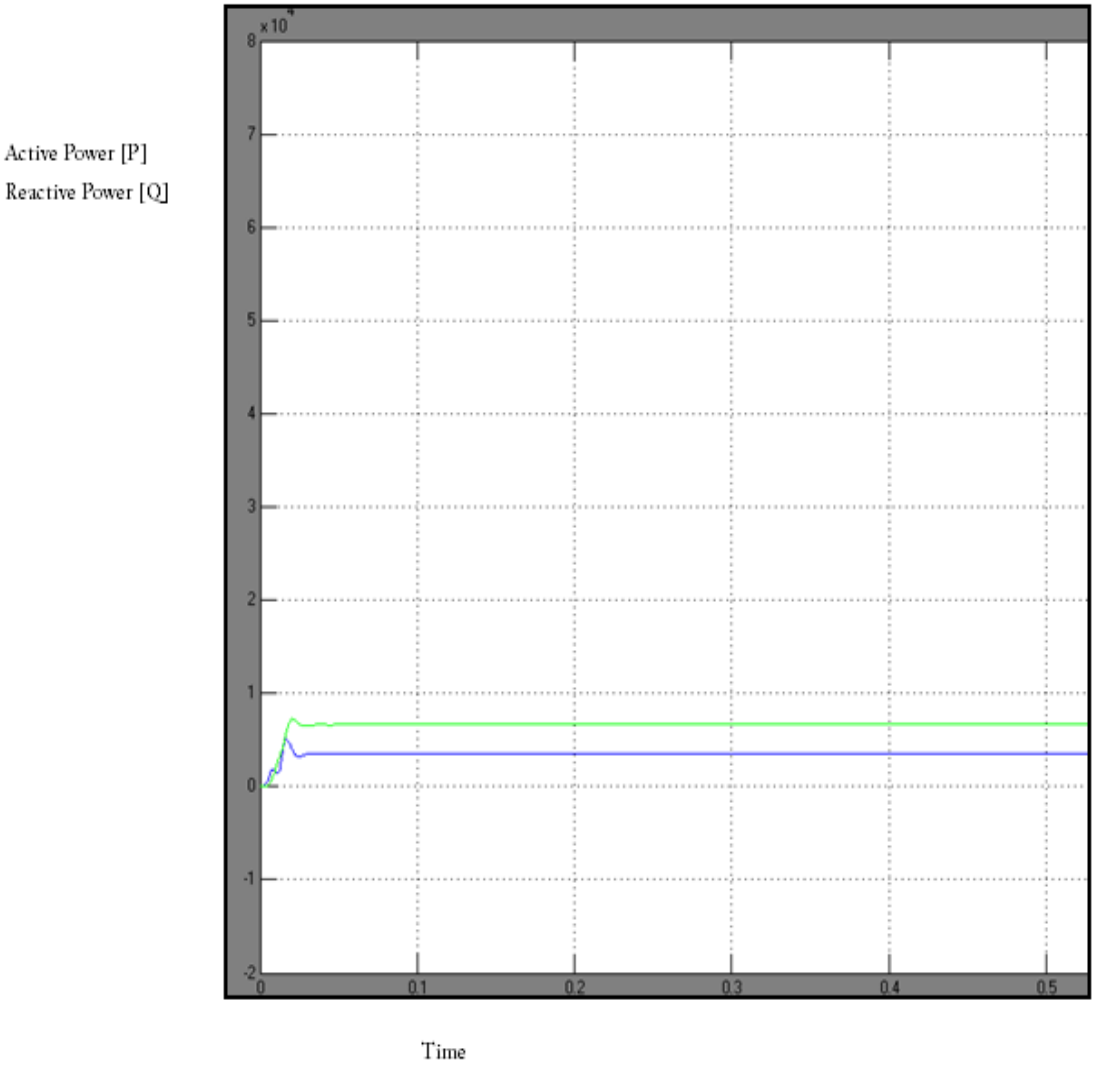

Figure 4.5. PQ waveform from the photo voltaic module/DC source.

The equivalent electrical circuit of a photo voltaic system connected to an inverter when its real and reactive power is measured is as shown below

With the sinusoidal waveforms, active power and reactive power signals observed from the DC supply, we now study the voltage and power supplied by the utility grid. All this observation is done when the entities are independent of each other and have not yet been connected.

4.3. Utility Grid

Utility grid in this thesis is a simple alternating current (AC) supply which is connected to one side of the load. A thevenin inductance (L) is connected in series with the utility grid.

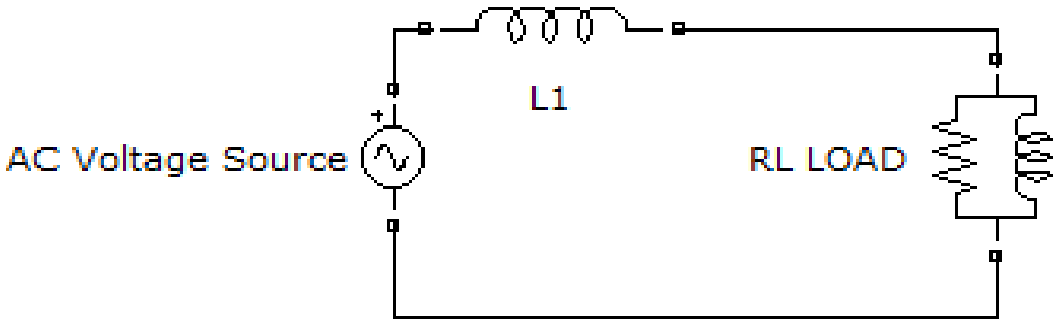

Figure 4.6: AC voltage source with Thevenin inductance connected to a RL load.

With AC voltage of 170 peak connected to a parallel RL load through a thevenin inductance of L1 = 0.000065, the active power [P] and reactive power [Q] are measured across the load. With the RL load having values of active power [P]: 1000 W and reactive power [Q]: 500 Vars, the circuit is verified.

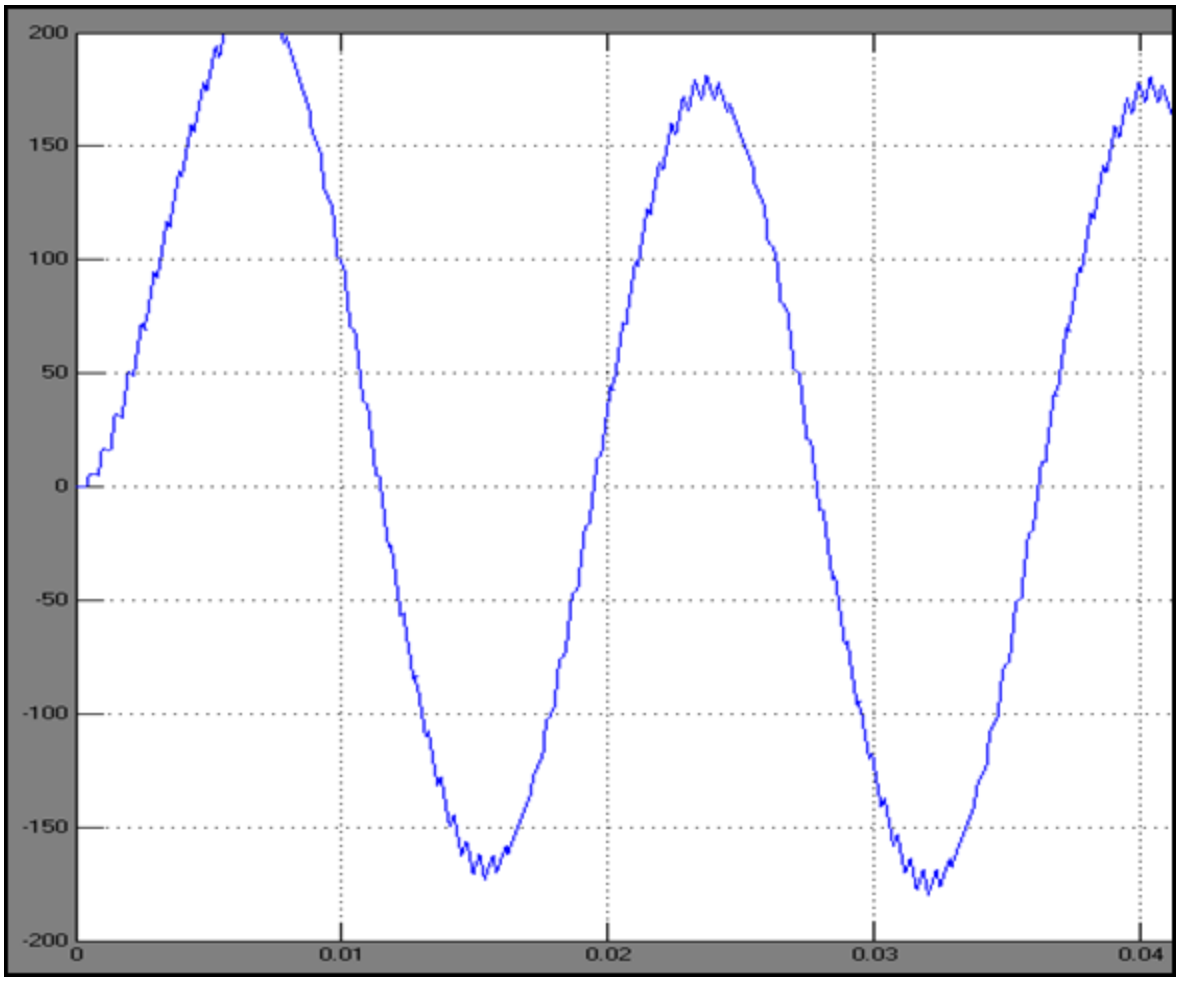

Figure 4.7: Voltage waveform from the Utility grid

The voltage being delivered by the utility grid is modeled such that its peak amplitude is 170 V, while the frequency is 60 Hz. The above waveform proves this statement. Now, the active power and the reactive power from the utility grid should be observed and noted so that when the load is connected to both the photo voltaic module and the utility grid it should have its power supplied simultaneously from both the sources with a certain split in them.

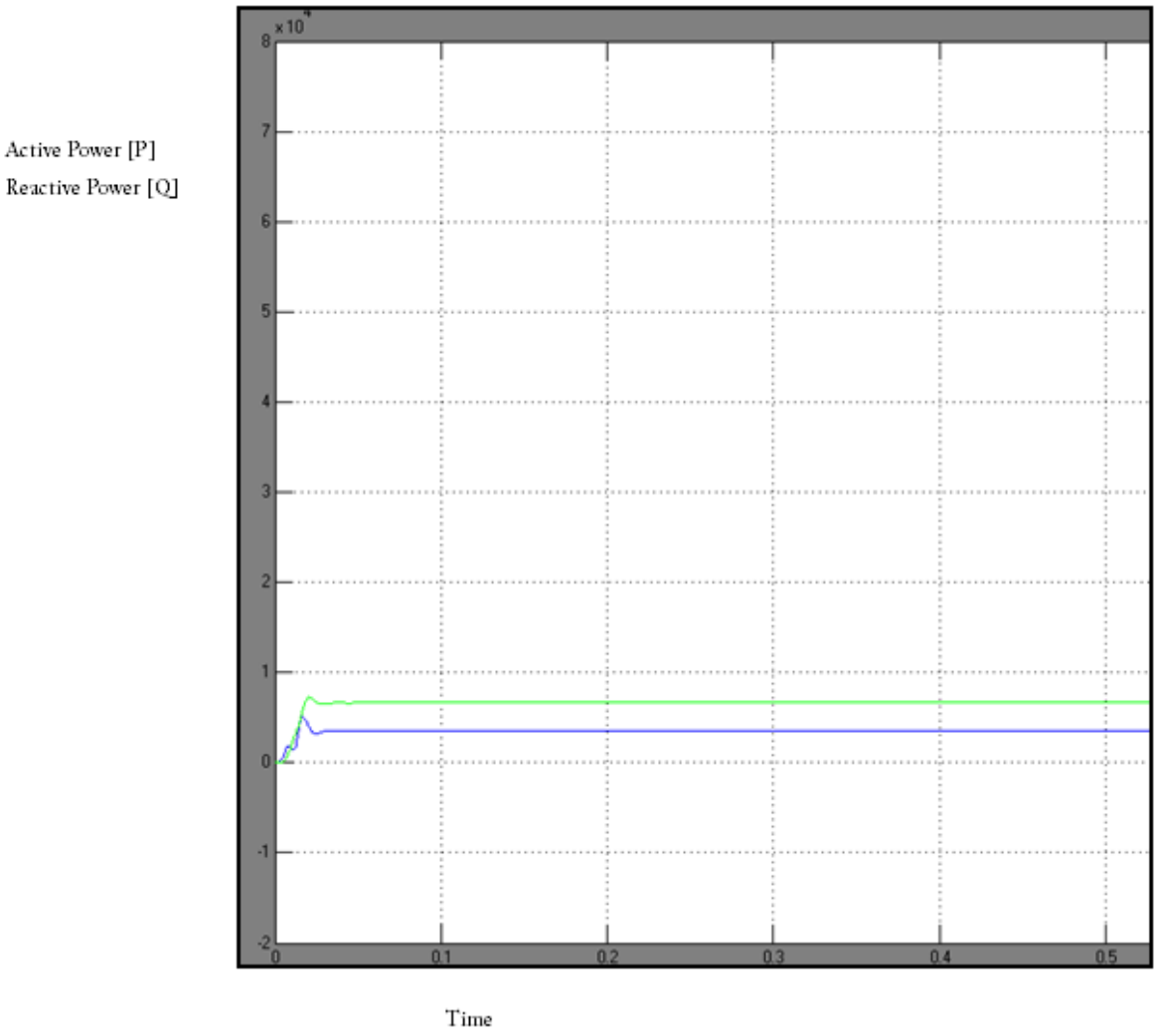

Figure 4.8: PQ waveform from the utility grid.

From the above waveform, we notice that the utility grid is supplying a smooth wave for both the active power and the reactive power.

4.4. Load connected to photo voltaic module and Utility grid

With above waveforms proving a smooth active power and reactive power being supplied by each of the sources, the main goal of this thesis was to observe the real and reactive power being consumed by the load when it is connected to both the supplies and perform transient analysis.

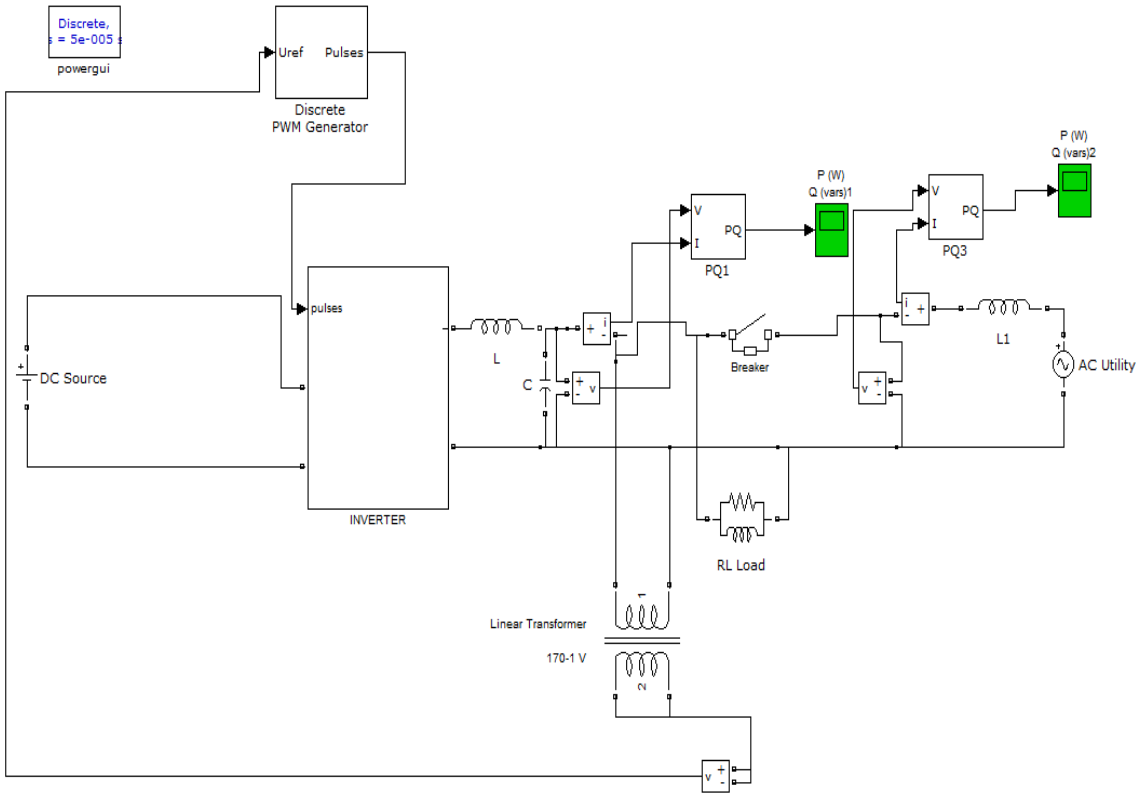

Figure 4.9 RL load connected to both DC source and AC utility grid.

The load as mentioned in previous chapters is a parallel Resistive (R) and Inductive (L) load. While one terminal is connected to the photo voltaic module, the other terminal is connected to the utility grid and under various conditions, analysis of the electrical system as a whole is performed.

As long as the voltage drawn by the load from the two electrical sources is constant inspite of varying condition, it can be asserted that the system is stable without any fluctuations in either frequency harmonics or the load voltage and load current . With these factors in ideal condition, the active power and reactive power also does not over load the system. It is understood that a basic model of microgrid has been developed in

this thesis and therefore there is an immense scope of further development to be carried out on a path of most ideal smart grid technology.

For the simulation, the RL load is specified to draw active power [P]=100e03 and reactive power [Q]=50e03. Therefore this total amout of active power and reactive power is split between the dc-inverter side and the AC utility side. The graphs below display this division of power between the two sources.

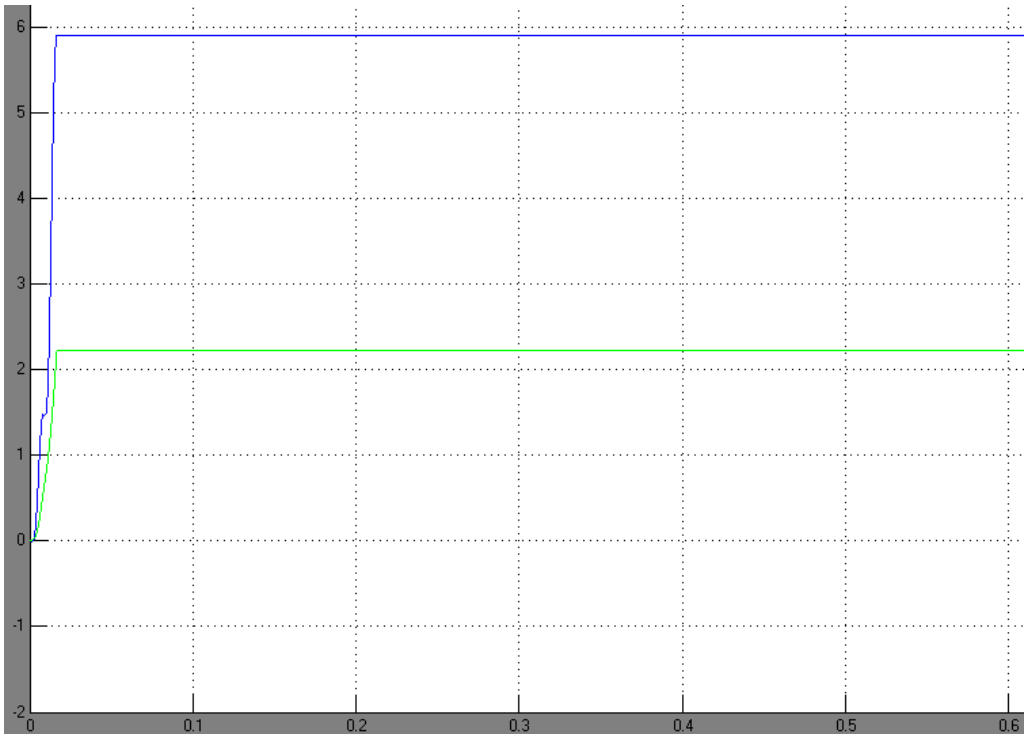

Figure 4.10: Graph showing the active power [P]= 59e03 and reactive power [Q]= 22e03 supplied by the utility AC.

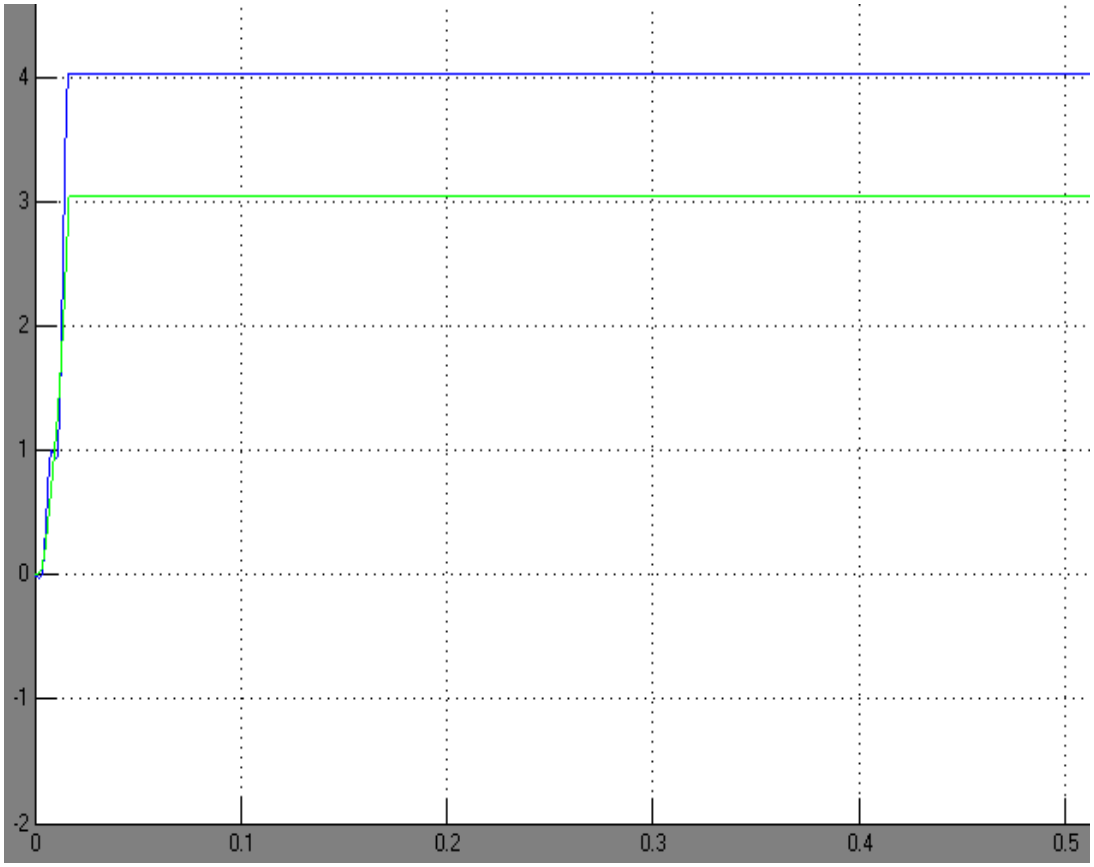

Figure 4.11 Graph showing the active power [P]=41e03 and reactive power [Q]=30e03 supplied by the DC source.

From the above two graphs, it can be observed that the active power and reactive power were shared equally by two sources. Therefore, it can be noted that the distributed generation model was developed well and its characteristics were same as discussed theoretically in the previous chapters.

4.5. Introduction of Islanding Phenomenon

One of the obstacles for the widespread application of photovoltaic (PV) systems in power networks is concern over islanding, i.e., when the disconnected part of the power network is sustained by the connected PV systems for a significant period of time.

Islanding must be avoided for several reasons including, the creation of a hazard for utility line workers by touching a line that should be otherwise de-energized, lack of control over voltage and frequency in the island, and interference with restoration of normal service.

In response to the above concern, PV inverter manufacturers now market the so-called “non-islanding” inverters that are expected to meet current interconnection standards. According to IEEE Std. 1547, these non-islanding inverters are expected to disconnect within 0.16 seconds, or 10 cycles, if the voltage drops below 50% or rises above 120% of its nominal value. The same maximum clearing time applies if the frequency drops below 59.3 Hz or rises above 60.5 Hz (based a 60 Hz nominal value). If the voltage drops to a value between 50% and 88%, or rises to a value between 110% and 120% of the nominal value, the allowed clearing time is expanded to 2 seconds, and 1 second, respectively.

Standard protection of grid-connected PV systems consists of four relays: over-voltage relay, under-voltage relay, over-frequency relay, and under-frequency relay. These relays will prevent islanding under most circumstances, as they disconnect the PV system from the utility in the event that the magnitude or frequency of the inverter's terminal voltage falls outside specified limits. However, if the local load closely matches the power produced by the inverter, the resulting deviations in voltage and/or frequency after a power outage may be too small to detect, i.e., fall within the non-detection zone. In this case, additional passive or active schemes are required to minimize the probability of an island to occur.

In this thesis we first review the standard protection against islanding based on detection of voltage and/or frequency deviations. The magnitudes of these deviations are derived for constant impedance loads in terms of active and reactive power mismatch coefficients. This is followed by the review of some of the most popular additional passive as well as active schemes that have been proposed to further reduce the possibility of islanding. Then an islanding test that was conducted on local grid-connected PV systems is described. Test results for cases where the PV systems generate (a) less power, (b) equal power, and (c) more power than the local load are presented and discussed. It is found that both grid-tied inverters satisfied the required standards in terms of run-on time.

4.6 Review of Anti-islanding Techniques

It has been reported that grid-tied PV systems normally operate at or near unity power factor, and this makes sense from an economic point of view. To settle such uncertainty, several local systems have been tested and they were found to operate between 98% and 99% power factor leading. So while the above statement can be considered correct, nonetheless, PV inverters do generate a small amount of reactive power that cannot be ignored in an island condition.

Consider Fig. 4.9 where a PV system is tied to the local grid under the presence of a local load. For simplicity, the load is considered of constant impedance type (i.e., a parallel R-L circuit) that consumes P_L watts and Q_L vars. The active and reactive powers generated by the PV system are denoted by P_D and Q_D, respectively. The utility system is shown to supply P_S watts and Q_S Vars. These powers are related as follows:

$$P_D + P_S = P_L \quad (1)$$

$$Q_D + Q_S = Q_L \quad (2)$$

Let the ratio of $P_S/P_D = \alpha$, and $Q_S/Q_D = \beta$. Then the above equations can be rewritten as

$$P_D(1+\alpha) = V^2 / R \quad (3)$$

$$Q_D(1+\beta) = V^2 / \omega L \quad (4)$$

where V and ω represent is the voltage at the interconnection point and system angular frequency, respectively.

When the utility disconnects, both P_S and Q_S go to zero and the voltage and frequency (V, ω) will settle to new values (V', ω'). These new values are related to the original ones the following equations:

$$V' = \frac{1}{\sqrt{1+\alpha}} V \quad (5)$$

$$\omega' = \frac{1+\beta}{1+\alpha} \omega \quad (6)$$

The above expressions show that the deviations in voltage and frequency depend on the level of power mismatch as well as direction of P_S and Q_S. Possible combinations are listed below:

Case A: $P_S > 0$ and $Q_S > 0$: The voltage decreases. The frequency depends on the values of α and β. If $\alpha = \beta$, then the frequency remains the same. If $\alpha > \beta$, the frequency increases. If $\alpha < \beta$, the frequency decreases.

Case B: $P_S > 0$ and $Q_S < 0$: Both the voltage and frequency decrease.

Case C: $P_S < 0$ and $Q_S > 0$: Both the voltage and frequency increase.

Case D: $P_S < 0$ and $Q_S < 0$: The voltage increases. The frequency depends on the values of α and β. If $\alpha = \beta$, then the frequency remains the same. If $\alpha > \beta$, the frequency increases. If $\alpha < \beta$, the frequency decreases.

Case E: $P_S = 0$ and $Q_S \neq 0$: The voltage remains constant, while the frequency changes (i.e., decreases if $Q_S < 0$ or increases if $Q_S > 0$).

Case F: $P_S \neq 0$ and $Q_S = 0$: The frequency remains constant, while the voltages changes (i.e., increases $P_S < 0$ or decreases if $P_S > 0$).

Case G: $P_S = 0$ and $Q_S = 0$: Both the voltage and frequency remain constant.

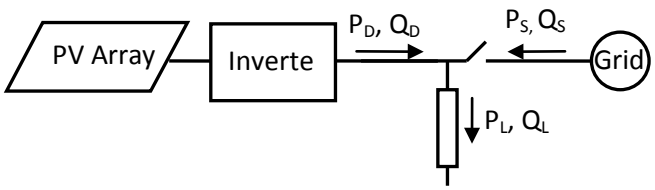

Figure 4.12 Grid-connected PV system with local load

Note that one of the over-voltage, under-voltage, over-frequency, or under-frequency relays will sense the voltage and/or frequency change in Cases A through F, hence preventing islanding. In Case G where the PV power production matches the load power requirement, however, none of these relays will operate since no change occurs in voltage and frequency. In reality, P_S and Q_S do not have to be exactly zero for this to occur because the magnitude and frequency of the utility voltage are expected to deviate slightly from nominal values. Therefore, the thresholds for the four relays cannot be set arbitrarily small or else the PV system will be subject to nuisance trips. This limitation leads to the formation of the so-called "Non Detection Zone". It is therefore important that PV systems incorporate ways to prevent islanding in the case where P_S and Q_S are very small. Some common methods for islanding prevention under such cases include the following:

a) *Voltage harmonic monitoring*, where the inverter monitors the voltage total harmonic distortion and shuts down if this parameter exceeds some threshold.

b) *Phase jump detection*, where the phase between the inverter's terminal voltage and its output current is monitored for sudden jumps.

c) *Slide-mode frequency shift*, where the current-voltage phase angle of the inverter is made to be a function of the system frequency.

d) *Impedance measurement*, where a perturbation is periodically applied to the inverter output current. If the utility is disconnected, this variation will force a detectable change in voltage which can then be used to prevent islanding.

e) *Active frequency drift*, where the inverter uses a slightly distorted output current to cause the frequency of the voltage to drift up or down when the utility is disconnected.

It is worth stating that none of the above methods works perfectly under all possible conditions, and each has advantages and disadvantages in terms of ease of implementation and associated cost, level of effectiveness, ease of selecting trip threshold, and power quality (i.e., spikes and waveform distortion).

4.7. Islanding Simulation and Field Test Results

Based on the MATLAB model described in earlier chapters, the different scenarios are simulated to verify the conclusions on circuit behavior and islanding phenomena.

Case A: $P_S>0$, $Q_S>0$:

The grid-tied PV system is constructed as described in previous chapter. In the model, the load is set as P_L= 8kW and Q_L= 2kVar at nominal voltage and frequency. And the PV panel's output is set as P_D = 7kW, and Q_D = 0. Thus, we can easily know that in steady state, P_S=1kW and Q_S=2kVar.

The simulation set the scenario as that the grid is disconnected at 1s. With the relay set to non-function, which means the PV panel is always connected to the load. The output voltage (RMS value), frequency and real and reactive power is shown in fig. 4.20.

Compared to the analysis previous chapter, the dynamics of voltage and frequency are the same. Note that the frequency increases to infinity slowly because the output reactive power of PV system should be zero at steady-state.

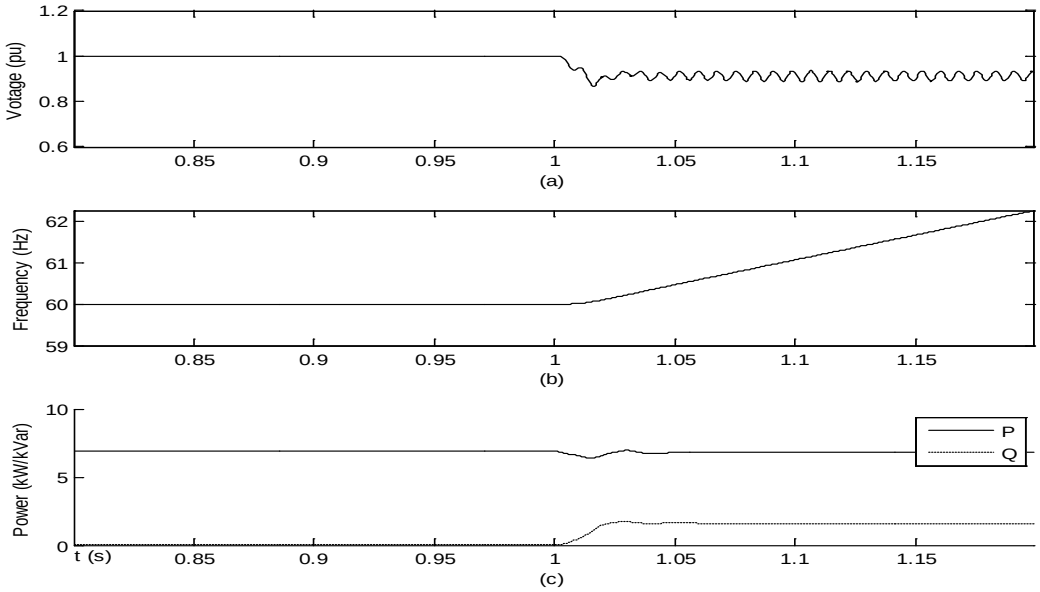

Fig. 4.13. Inverter Terminal Voltage, Frequency & Output Real and Reactive Power

(With relay set to non-function)

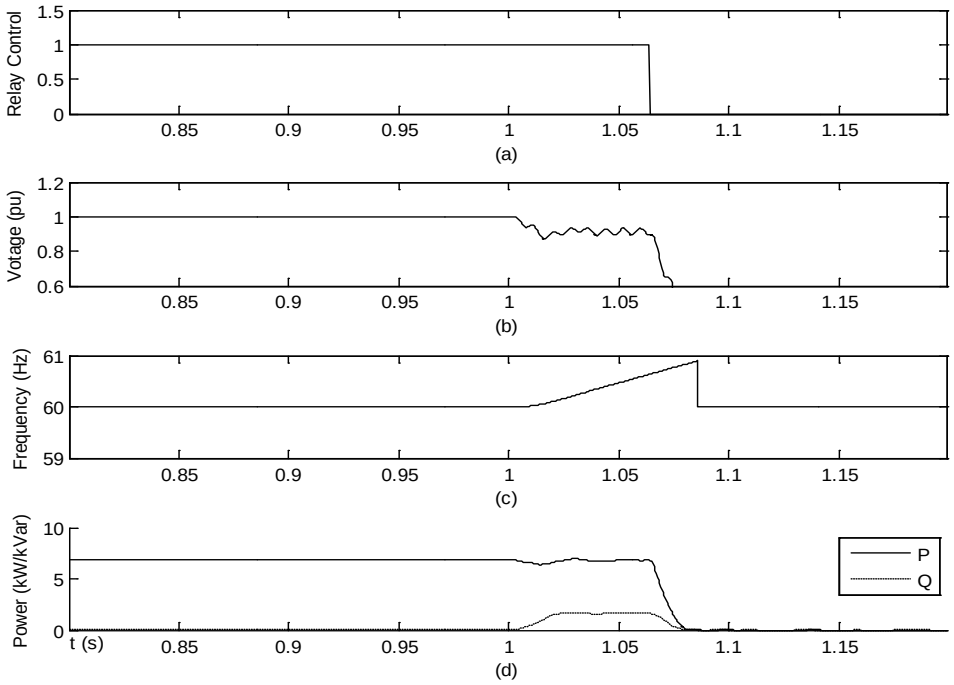

Fig. 4.14. Inverter Terminal Voltage, Frequency & Output Real and Reactive Power and Relay Control Signal (With relay set to function)

The relay control signal shows the relay respond at about 0.07s, which is about 4-5 cycles, after the disconnection of the grid happens.

Case B: $P_S>0$, $Q_S<0$:

The grid-tied PV system is constructed as described in earlier chapter. In the model, the load is set as $P_L = 8$ kW and $Q_L = -2$ k Var at nominal voltage and frequency. And the PV panel's output is set as $P_D = 7$ kW, and $Q_D = 0$. Thus, we can easily know that in steady state, $P_S=1$kW and $Q_S=-2$kVar.

The simulation shows that in this case the output voltage and frequency both drop after the disconnection of the grid, which is consistent with the analysis presented in the earlier chapter.

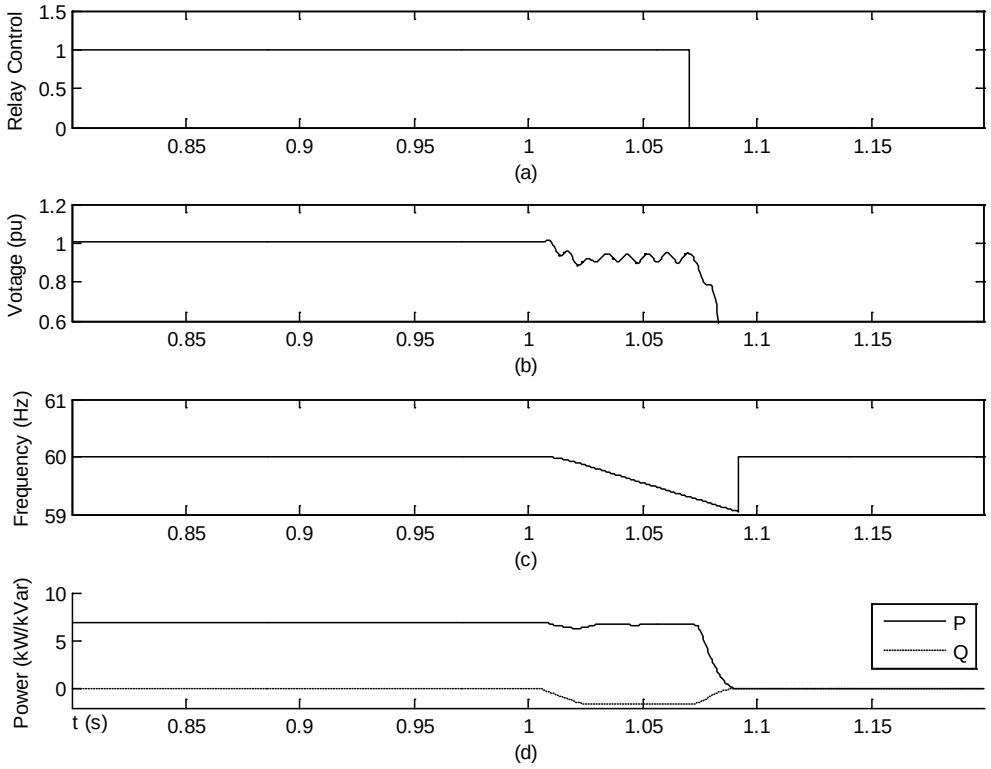

Fig. 4.15. Case B, Inverter Terminal Voltage, Frequency & Output Real and Reactive Power

and Relay Control Signal (With relay set to function)

Case C: $P_S<0$, $Q_S>0$:

In the model, the load is set as P_L=8kW and Q_L=2kVar at nominal voltage and frequency. And the PV panel's output is set as P_D=9kW, and Q_D=0. Thus, we can easily know that in steady state, P_S=-1kW and Q_S=2kVar.

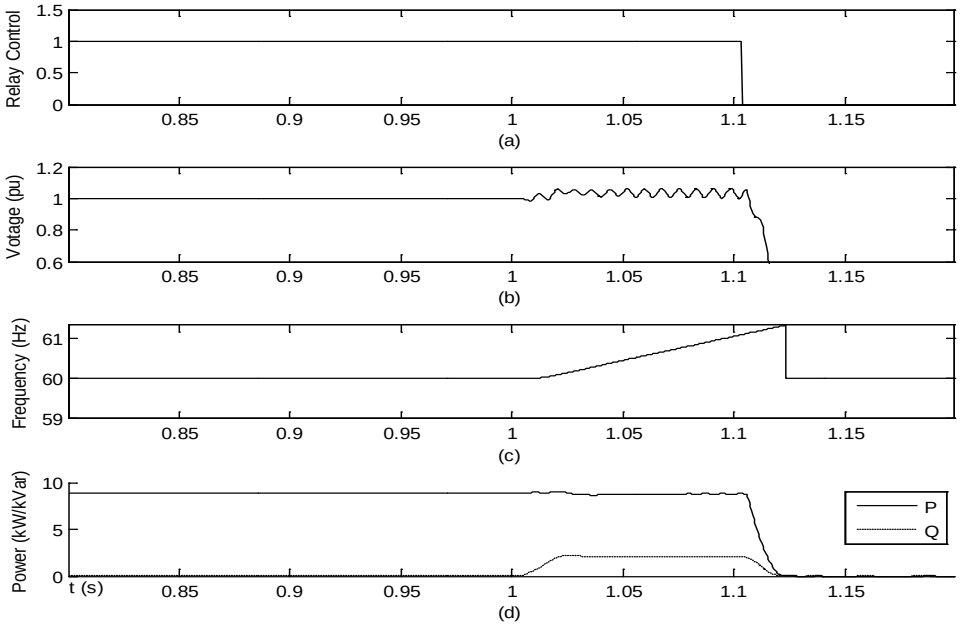

Fig. 4.16 Case C, Inverter Terminal Voltage, Frequency & Output Real and Reactive Power and Relay Control Signal (With relay set to function)

The simulation shows that in this case the output voltage and frequency both increases after the disconnection of the grid, which is consistent with the analysis in earlier chapter.

Case D: $P_S<0$, $Q_S<0$:

The grid-tied PV system is constructed as described in previous chapter. In the model, the load is set as P_L=8kW and Q_L=-2kVar at nominal voltage and frequency. And the PV panel's output is set as P_D=9kW, and Q_D=0. Thus, we can easily know that in steady state, P_S=-1kW and Q_S=-2kVar.

The simulation shows that in this case the output voltage increases and frequency drops after the disconnection of the grid, which is consistent with the analysis in previous chapter.

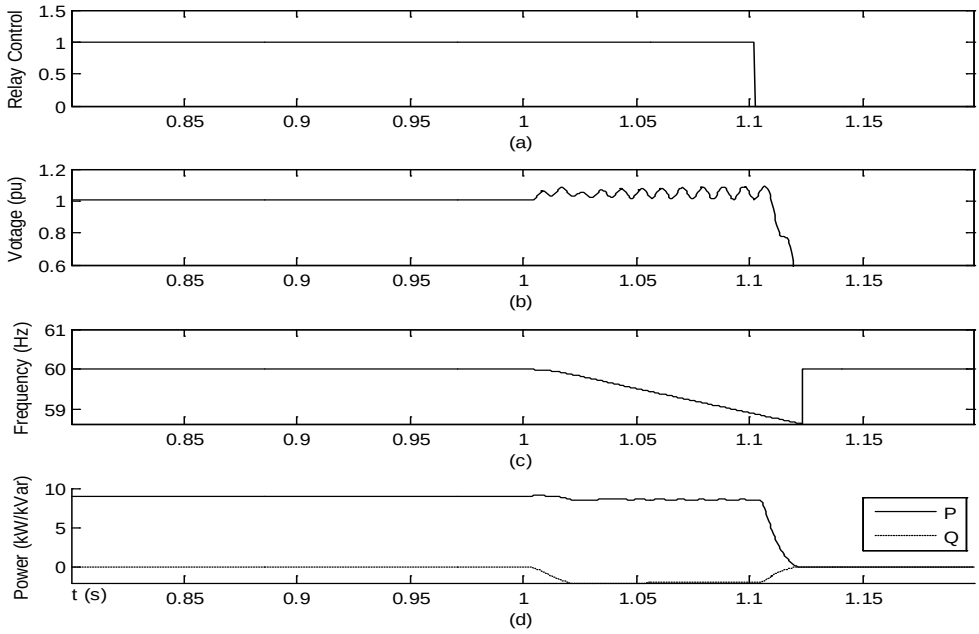

Fig. 4.17 Case D, Inverter Terminal Voltage, Frequency & Output Real and Reactive Power

and Relay Control Signal (With relay set to function)

Case E: P_S=0, Q_S=0:

The grid-tied PV system is constructed as described as in previous chapter. In the model, the load is set as P_L=8kW and Q_L=0 at nominal voltage and frequency. And the PV panel's output is set as P_D=8kW, and Q_D=0. Thus, we can easily know that in steady state, P_S=0 and Q_S=-2kVar. According to the analysis in Chapter 3, this will result in no or little difference on output voltage and frequency. And in such case, the islanding phenomenon appears.

The simulation shows that the output voltage and frequency both are almost the same as those before the disconnection of the grid, which is consistent with the analysis in earlier chapter. And the relay doesn't act because it couldn't sensor any difference between before and after the disconnection of the grid. And the simulation shows the islanding phenomenon successfully.

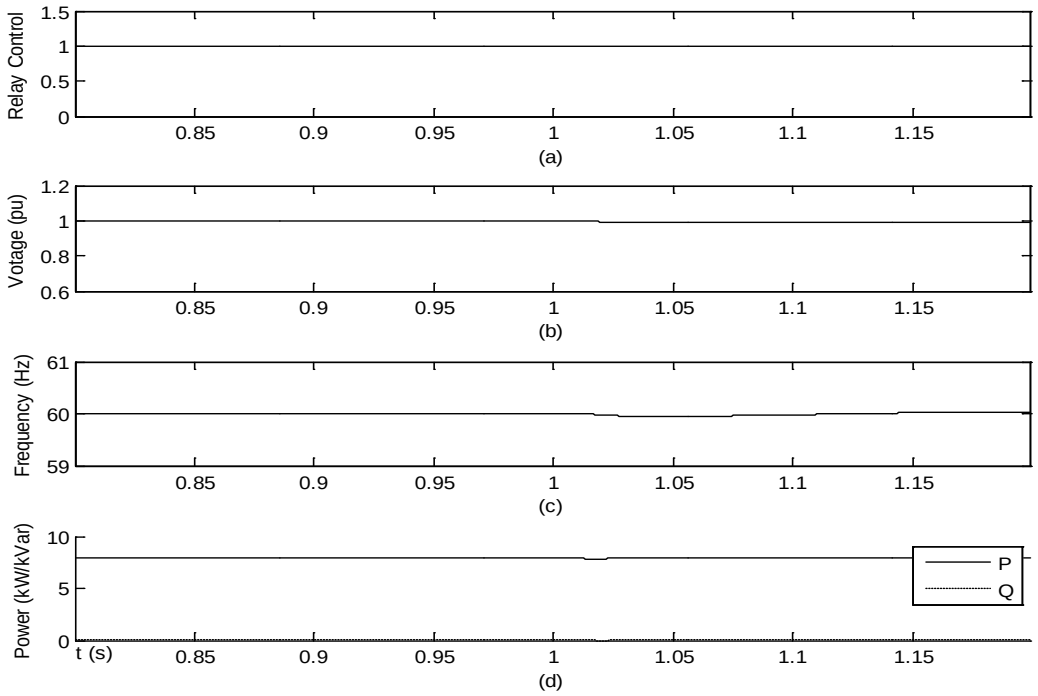

Fig. 4.18 Case E, Inverter Terminal Voltage, Frequency & Output Real and Reactive Power and Relay Control Signal

CHAPTER 5

Conclusion and Future Scope

The islanding of photovoltaic installations has been considered in the past as a major concern over the safety of utility personnel. Nowadays, grid-tie inverters are designed such that they effectively disconnect from the grid immediately after a utility disturbance in either frequency of voltage takes place. In this thesis we reviewed the standard anti-islanding protection by four commonly used relays and various additional schemes that tend to minimize the non-detection zone. All existing methods involve a tradeoff between effectiveness in islanding prevention, power quality, simplicity and cost-effectiveness.

This thesis also reported the results of an islanding test that was conducted on two PV systems under various levels of load matching to PV generation using a load bank. The captured voltage waveforms immediately after utility disconnect clearly show the expected variations in both magnitude and frequency. It was determined that both systems shut down in less than 5 cycles (or 0.08 seconds) after a utility outage, thus exceeding the recommended standards for islanding.

To analyze the dynamic performance of Microgrids, proper dynamic models are required for different investigation purposes. Therefore, component models, which reflect the physical processes within Microgrid components, are modeled to simulate the dynamics of Microgrids for steady-state studies and transient analysis. In this thesis, modeling of components of a microgrid system has been successfully done. Models, which allow the investigation of the individual power sources behavior, have been developed. Testing was also a significant part of this study. The future study lies in the fact that with further development carried out on the system, with the goal of microgrids

being able to generate power in an economical and efficient way by reducing the costs and the emission can certainly be achievable. Although certain components were specifically chosen, the models are easily generalizable to other, similar components.

REFERENCES

[1] Anca D. Hansen, Paul Sorensen, Lars H.Hansen and Henrik Binder, “Models for stand alone PV systems”, Riso National Laboratory, Roskilde, December 2000.

[2] Lorenzo, E. “Solar Electricity Engineering of Photovoltaic Systems”,S.L., Spain, 1994.

[3] Takashi Ishikawa, Kosuke Kurokawa, “Evaluation of operation characteristics in multiple interconnection of PV systems”, In: Technical digest of the international PVSEC-12, Korea; 2001.

[4] Y. Baghzouz, “Effect of Grid-Tied Photovoltaic Systems of System Reliability and Peak Demand”, International Conference on Energy and Sustainable Developments, Phuket, Thailand, March 1-3, 2006.

[5] Nattapong Chayawatoo, Krissanapong Kirtikara, Veerapol Monyakul, Chiya Jivacate, Dhiryacut Chenvidhya, “DC-AC switching converter modeling of a PV grid connected system under islanding phenomena”, Renewable energy, Science direct, 9 June 2009.

[6] Kobayashi Hiromu, Takigawa Kiyoshi, “Statistical evaluation of optimum Islanding preventing method for utility interactive small scale dispersed PV systems”, IEEE; 1994.

[7] Ljung, L, “System Identification Toolbox- for use with Matlab”, 6 edition, The Math Works, Inc, 2000.

[8] Smith GA, Onions PA, Infield DG. “Predicting islanding operation of grid connected

“PV inverters”, IEEE Procedural Electrical Power Applicaton 2000 January; 147.

[9] Ian A. Hiskens Eric M. Fleming, p. 405–6, “Control of Inverter-Connected Sources in Autonomous Microgrids”, Department of Electrical and Computer Engineering University of Wisconsin – Madison, Madison, WI 53706 USA., 2005.

[10] M. B. Bana Sharifian, Y. Mohamadrezapour, M. Hosseinpour and S. Torabzade, “Single State Grid Connected Photo voltaic System with Reactive Power control”, Department of Electrical and Computer Engineering, University of Tabriz, Tabriz, Iran, 2009.

[11] Woyte Achim, Belmans Ronnie, Jijs Johan “ Testing the islanding protection function of photovoltaic inverters”, IEEE Trans Energy Convers March 2003;18(1):157–62

[12] Liu Yan-Fei, Sen Paresh C. “A large-signal model for current-programmed boost converter”, IEEE; 1994.

[13] SimPowerSystem, MATLAB.

[14] J.Nagarjuna Reddy, M.Kalia Moorthy, D.V. Ashok Kumar, “Control of Grid Connected PV Cell Distributed Generation Systems”, IEEE Trans, 2005.

[15] Oystein Ullberg, “Stand Alone Power Systems for the future optimal Design, Operation and Conrol”, Ph.D Dissertation, Norwegian University of science and technology, Trondheim 1998.

[16] T.U. Townsend, “A methold for estimating the long term performance of direct coupled photo voltaic systems”, MS thesis, University of Wisconsin, Madison, 1989.

[17] Smith J.H and Reiter L.R, “An In-depth Review of Photovoltaic system performance models, The American Society of Mechanical Engineers, 84-WA/Sol-12, 1984.

[18] R.D. Middle Brook, “Small Signal modeling of pulse width modulated switched mode power converters”, Proceedings of IEEE, Vol 76, No 4, pp 343-354, April 1988.

[19] A. Kisiovski, R. Redl and N. Sokal, “Dynamic analysis of switching-mode DC/DC converters”, New York: Van No strand Reinhold, 1994.

[20] “POWER ELECTRONICS – Converters, Applications and Design”, Mohan, Under land, Robbins, John Wiley & Sons.

[21] “POWER ELECTRONICS – Circuits, Devices and Applications”, Muhammad H. Rashid, Prentice hall of India Private Limited.

[22] W. Shireen and M. S. Arefeen, “An utility interactive Power electronics interface for alternate/renewable energy systems”, IEEE Trans. Energy Conversion, Vol 11, No:3, pp 643-649, Sept 1996.

[23] “Voltage Stability of Electric Power Systems” – Thierry Van Cutsem, Costas Vournas, Power Electronics and Power Systems Series.

[24] Chensong Dai, Y. Baghzouz, “Microgrid Islanding”, IEEE, March 2005.

[25] IEEE Std. 929-2000, Recommended Practice for Utility Interface of Photovoltaic (PV) Systems, IEEE Press, 2000.

[26] John Stevens, Russell Bonn, Jerry Ginn, and Sigifredo Gonzalez, "Development and Testing of an Approach to Anti-Islanding in Utility-Interconnected Photovoltaic Systems", Sandia National Laboratories, *Report* No. SAND 2000-1939, August 2000.

[27] S. Gonzalez, R. Bonn, and J. Ginn, "Removing Barriers to Utility Interconnected Photovoltaic Inverters", Proc. 28th IEEE Photovoltaic Specialist Conference, Anchorage, AK, Sept 15-22, 2000.

[28] IEEE Standard. 1547, Standard for Interconnecting Distributed Resources with Electric Power Systems, IEEE Press, 2003.

[29] A. Ye, A. Kolwalkar, Y. Zhang, P. Du and R. Walling, "Evaluation of Anti-Islanding Schemes Based on Non-detection Zone Concept", IEEE Trans. Power Electronics, Vol. 19, No. 5, Sept. 2004, pp. 1171-1176.

[30] M.E. Ropp, K. Aaker, J. Haigh, N. Sabbah, "Using Power Line Carrier Communications To Prevent Islanding", Proc. 28th IEEE Photovoltaics Specialists Conference, Sept. 17-22, 2000, p. 1675-1678.

[31] T. Ishida, R. Hagihara, M. Yugo, Y. Makino, M. Maekawa, A. Takeoka, R. Susuzi, S. Nakano, "Anti-Islanding Protection Using a Twin-Peak Band-Pass Filter in Interconnected PV Systems, and Substantiating Evaluations", 24th IEEE Photovoltaics Specialists Conference – 1994, Dec. 5-9, 1994, p. 1077 –1080.

[32] M.E. Ropp, M. Begovic and A. Rohatgi, "Prevention of Islanding in Grid-tied Photovoltaic Systems", Progress in Photovoltaics Research and Applications, Vol. 7, 1999, pp. 39-59.

[33] M. Begovic, M. E. Ropp and A. Rohatgi, “Determining the sufficiency of standard protective relaying for islanding prevention in grid-connected PV systems”, Proc. 2nd World Conference on Photovoltaic Energy Conversion, Vienna, Austria, May 1998.

VITA

Graduate College
University of Nevada, Las Vegas

Chandu Venu

Degrees:

Bachelor of technology, Electronics and Communication Engineering, 2007
Jawaharlal Nehru Technological University, Hyderabad, India.

Thesis Title:

Islanded Operation of a Distribution Feeder with Distributed Generation

Thesis Examination Committee:

Chairperson, Dr. Yahia Baghzouz, Ph.D, PE
Committee Member, Dr. Paolo Ginobbi, Ph.D
Committee Member, Dr. Yingtao Jiang, Ph.D
Graduate Faculty Representative, Dr. Laxmi P. Gewali, Ph.D